University of Padua

Department of Physics and Astronomy

Master Thesis in Physics

Emergent of Criticality in Living Systems

Supervisors

Professor Amos Maritan
University of Padua

Professor Samir Simon Suweis
University of Padua

Master Candidate

Andrea Veronese

Academic Year

2022-2023

Dedication.

I would like to dedicate this thesis to my parents who have always been understanding and have supported me through my education.

Abstract

The hypothesis that complex interacting living systems can benefit from operating at the vicinity of critical points has gained momentum in recent years. Criticality may confer an optimal balance between too ordered and exceedingly noisy states. In this thesis we will study a model, based on information theory and statistical mechanics, illustrating how and why a community of agents aimed at understanding and communicating with each other converges to a globally coherent state in which all individuals are close to an internal critical state, i.e. at the borderline between order and disorder. We will study both analytically and computationally the circumstances under which criticality is the best possible outcome of the dynamical process, and eventually confirming the convergence to critical points under very generic conditions. Furthermore the effect of evolutionary strategy will be investigated together with the role of different time scales in evolution and adaptation.

Contents

Listing of figures

Listing of tables

Introduction

Several studies ([1], [2], [3], [4]) has pointed out that living systems could operate in proximity of critical points similar to the well-known ones found in the study of phase transitions in statistical physics. Indeed, it appears that a whole class of examples, ranging from spontaneous brain behavior [5] to gene expression patterns [6], cell growth [7], morphogenesis [8], bacterial clustering [9], flock dynamics [10] and many more, suggests that interacting living systems have a tendency to behave as if they were close to a "border line" between an ordered and a disordered phase, as it happens with correlated spin in a magnet at the point of ordering. Even if none of these examples is fully conclusive and even if the meaning of "criticality" varies across these works, the criticality hypothesis, as a general strategy for the organization of living matter, is a tantalizing idea worthy of further investigation.

Although different mechanisms and scenarios have been described in the recent literature, a complete theory that explains why and how interacting living systems arrange themselves in this particular manner is still missing. As a matter of fact, critical points, with all their remarkable properties ([11], [12]), are only observed upon fine tuning of the macroscopic parameters of the system in a small region around the critical point of interest. This is in sharp contrast to the ubiquity of critical-like behavior in complex living matter. Nevertheless, in a study from 2014 by *Hidalgo et al.* [13] criticality has been shown to arise in communities of agents which seek to interpret and model as efficiently as possible external information they receive from the environment; suggesting, also, that the drive to criticality comes from functional advantages of being poised in the vicinity of a critical point.

In particular, this approach describes the environment as a set of information sources each consisting of an individual from the population under examination; each individual of the community tries to mimic, i.e. to infer or "understand", the state of others within a community. Under this dynamics, it is possible to observe that the community experiences a drift toward the critical point of the dynamics, i.e. at the edge between an ordered and disordered phase. Remarkably enough, this emerging criticality involves a large variability among individuals; indeed, when the system is in the critical regime, it can be observed that small variations in parameter values are reflected in large state changes, suggesting, somehow surprisingly, that individuals aiming at understanding each other in the best possible way end up exhibiting a

large variability.
In this thesis we will study and analyze both analytically and computationally the circumstances under which criticality is the best possible outcome of the dynamical process, and eventually confirming the convergence to critical points under very generic conditions. More specifically, we will use ideas from information theory and statistical mechanics to build a general framework which shows why and how criticality is the optimal strategies a community of agents could take in order to overcome efficiently external stimuli. Furthermore, following the ideas of the paper from 2016 by *Hidalgo et al.* [14], we will investigate also the role of evolutionary strategy - i.e. evolutionary behaviour that changes the process of information transfer by altering the way each individual approach its fitness into the community - exploring whether or not there's an one and what consequences it has on the evolution of the system.

The thesis is organized as follows:
In Chapter 1 we will expound on the subject of criticality in statistical mechanics and we will present the reader with several examples of critical phenomena in biological systems.
In the following Chapter 2 we will introduce the reader a framework to study criticality in living systems. In particular, we will describe the model presented by *Hidalgo et. al* [13] and extend upon it.
We will then present, in Chapter 3, the results we obtained exploiting this model, focusing in particular on those obtained computationally from the generalisation of the original model.
In Chapter 4 we study and develop an analytical framework to study both criticality and strategy stability.
Finally, the last chapter will consist of a brief summary of the project, a discussion of our conclusions and future developments that this work may open up.

1

Statistical Physics of Living Systems

One of the biggest questions of our time concerns the understanding of the phenomenon we call ”life” with all the astonishing diversity and complexity it exhibits. From cells to multicellular organisms based on the perfect coordination of up to trillions of interacting molecules, to communities of individuals which interact in countless ways, forming entangled and complex ecosystems and giving rise to a hierarchy of complexity, questions such as “how are those myriads of elements and interactions coordinated together in complex living creatures?” or “how does coherent behavior emerge out of such a soup of highly heterogeneous components?” (Schrödinger, 1967[15]) rise naturally.

The standard point of view of biology is that each molecular component (protein, nucleic acid, metabolite, etc.) is specific and requires individualized analysis. This approach has successfully identified and quantified most of the components and many of the basic interactions of life as we know it. Still, unfortunately, it offers no convincing explanation of how systemic properties emerge.

An alternative strategy consists of looking at complex biological problems from a global perspective, shifting the focus from specific details of the molecular machinery to more collective behaviours. Systematic approaches to biology rely on the evidence that some of the most fascinating phenomena of living systems, such as memory and the ability to solve problems, are collective ones, rising from the interactions of many basic units and which might not be reducible to the understanding of elementary components on an individual basis. Theoreticians have long struggled to explain whether simple and general principles, such as those in physics,

could be of any help in tackling the complexity in living systems. More specifically, they have long been seduced by the idea of adapting concepts and methods from statistical mechanics to shed light onto the large-scale organization of interacting living systems.

1.1 Criticality in Equilibrium Systems

The concept of criticality and critical phenomena were born in the field of statistical physics of equilibrium. When talking about critical phenomena, we refer to certain particular properties a system exhibits in the proximity of its critical points. These points are generally associated with scale invariance and the divergence in the derivatives of some thermodynamic potential, e.g. susceptibility, specific heat, etc. Scale invariance and criticality translates into collective behaviour in many-body systems, which depend only on few aspects, such as dimensionality and system's symmetries.

A paradigmatic example is ferromagnets. These exhibit a continuous or second-order phase transition at a critical temperature T_c below which the orientational symmetry of spins is spontaneously broken, i.e., a preferred direction emerges, and progressively more ordered and magnetized states emerge as the temperature is lowered. On the other hand, above T_c thermal fluctuations dominate and the system remains disordered. This change in the collective state is usually encoded in an order parameter (e.g., the overall magnetization) which measures the degree of order as the phase transition proceeds.

The described symmetry breaking is a collective phenomenon that requires a system-wide coordination for the collective behaviour to emerge. This implies that the correlation length among individual components needs to span the whole system at criticality. Similarly, when the system is becoming incipiently ordered, it is highly fluctuating in the orientation to be chosen. Indeed, in the critical regime the system is highly susceptible to external perturbation, for example a magnetic fields will have little influence on the system at both low and high temperatures, whereas it is at criticality that it shows the greatest response; the magnetic susceptibility reaches a maximum at the critical point for finite-size systems and diverges for infinite ones.

Given the universality of critical behaviours and their dependencies on only few characteristics,it is possible to use Ising model to describe even more complex systems, without taking into account small and specific details since they do not play an important role in the reaching of a phase transition. Furthermore, the concepts and methods developed in the context of equilibrium systems were soon extended to time-dependent and non-equilibrium problems, which seem to be a more suited approach when analyzing living systems, which are dynamical entities

kept away from thermal equilibrium by permanently exchanging energy and matter with their surroundings.

1.2 Non-Equilibrium Phase Transitions

Non-equilibrium phase transitions has a much richer phenomenology than equilibrium phase transitions, because states lack a universal description in terms of thermodynamic potentials. From a methodological point of view, this situation results in a large variety of universality classes without general tools for their characterisation, hence it is not even obvious how to define a non-equilibrium phase transition.

For this reason, we limit our overview to directed percolation (DP), which is the prototypical example (universality class) of a phase transition in the presence of one single absorbing state. A simple model of such process is represented by a lattice where each site s_i can be either occupied/active ($s_i = 1$) or empty/quiescent ($s_i = 0$). An active site can "infect" a neighboring site if they are connected by an active bond. This model, called bond percolation, is well studied in equilibrium statistical physics, where it is known to be equivalent to a Potts model. In practice, each bond is made active with probability p, and for p larger than some critical value p_c there is an infinite cluster of active sites spanning the entire system (Fig. 1.1).

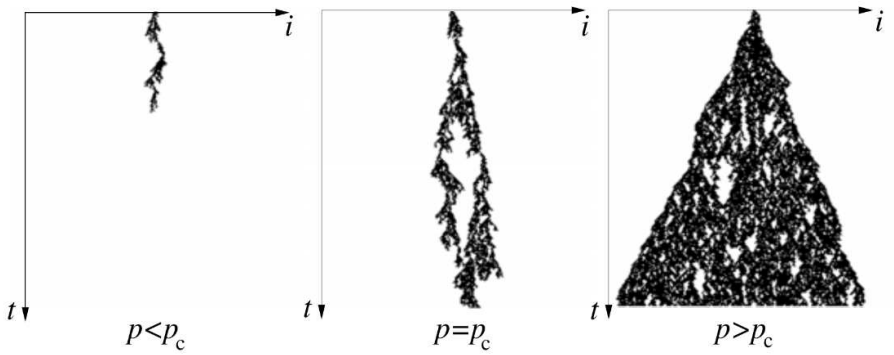

Figure 1.1: Typical DP clusters grown from a single seed in 1+1 dimensions below, at and above criticality. Below a certain well-defined threshold $p < p_c$ all generated clusters remain finite while for $p > p_c$ some of the clusters spread infinitely over the entire system. These two phases are separated by a sharp transition point at a specific critical threshold $p = p_c$ which in the case of bond DP in one space dimension is close to 0.6447

For value of p smaller than the critical threshold p_c, the system approaches a configuration without any active sites. Such a configuration, from where the system cannot escape, is called absorbing. More specifically, an absorbing state is a configuration that can be reached by the

dynamics but not be left by them. Therefore, DP is said to display a non-equilibrium phase transition from a fluctuating phase into an absorbing state or, more concisely, an absorbing phase transition.

It is instructive to study the average number of active sites $\langle N(t) \rangle$ (Fig. 1.2). It can be observed that at the critical value p_c, the average number of active sites follows a power law, which is indicative of the universal behaviour valid in the limit of large times t and for large system sizes.

As in equilibrium statistical mechanics, it turns out that continuous phase transitions in sys-

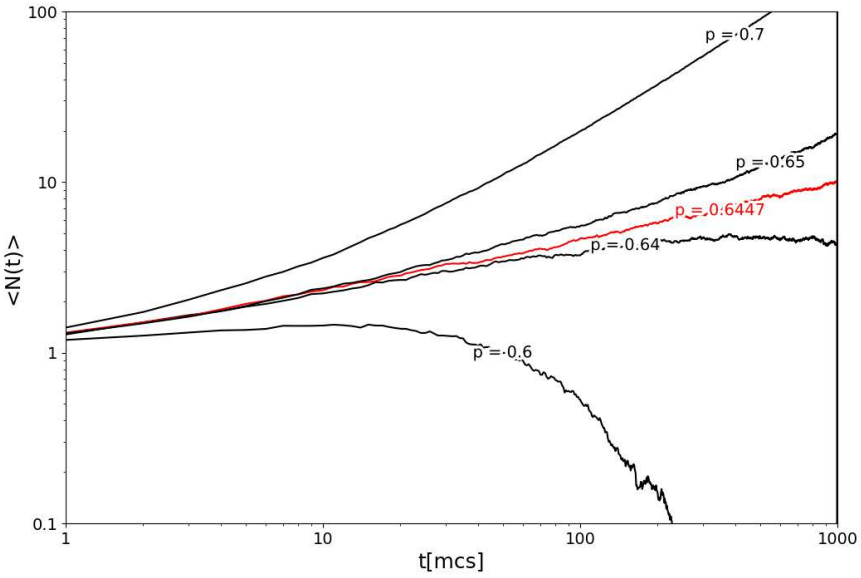

Figure 1.2: Average number of active sites $\langle N(t) \rangle$ as a function of time t (measured in units of Monte Carlo steps) for various percolation probabilities p. Below the critical threshold the average number of sites $\langle N(t) \rangle$ first increases until it crosses over to an exponential decay. Above the critical point the increase accelerates until it crosses over to a linear increase. Precisely at the critical point $p = p_c$ the corresponding curve in the log-log plot appears to be straight, indicating power-law behaviour

tems out of equilibrium can be grouped into universality classes which are associated with certain critical exponents (Table 1.1). As a result of universality, all models exhibiting a phase transition to an absorbing or quiescent phase share the same set of critical exponents and scaling functions, i.e., the same type of scale-invariant organization, with the DP process.

This turns out to be crucial for analyzing critical phenomena in living systems. Indeed - even though perfect power laws and divergences can appear only in the infinite-size limit, not reachable in biological problems - thanks to the aftermath of universality, these systems still may exhibit a progressive transition between order and disorder, which can be characterized by the existence of a peak in some quantity such as the susceptibility or the correlation length that

Exponent	$d = 1$	$d = 2$	$d = 3$	Mean Field
β	0.276	0.583	0.813	1
$\nu_\perp$	1.097	0.733	0.584	1/2
$\nu_\parallel$	1.734	1.295	1.110	1
θ	0.314	0.229	0.114	*not valid in the MF regime*

Table 1.1: Numerical and mean-field critical exponents for the DP universality class [16]. The exponent β describes the behaviour of the the density of active sites asymptotically, e.g. $\rho(\infty) \sim (p - p_c)^\beta$. The exponents $\nu_\perp$ and $\nu_\parallel$ describe the divergence of the spatial ($\perp$) and temporal ($\parallel$) correlation length close to criticality, e.g. $\xi_\perp \sim (p - p_c)^{-\nu_\perp}$, $\xi_\parallel \sim (p - p_c)^{-\nu_\parallel}$. Lastly, θ describe the asymptotic behaviour of the average number of active sites, e.g. $\langle N(t) \rangle \,|_{p=p_c} \sim t^\theta$

usually diverges at criticality.

1.3 Self-Organized Criticality

The critical phenomena showed up to now both of equilibrium and of non-equilibrium had the common feature that the fine tuning of a suitable order parameter was necessary in order to get a critical behavior, characterized by scale invariance. Then, how is it possible that living systems exhibit signatures of criticality, without the need, apparently, of any parameters' tuning to settle themselves at the edge of a phase transition?

Interestingly enough, it was discovered in some seminal papers by Per Bak and coworkers at the end of the 1980s ([17], [18], [19]) that there are driven-dissipative systems that spontaneously evolve toward a critical dynamics, characterized by a power-law distribution of relaxation events, and this phenomenon does not require the tuning of any parameter, hence it is named self-organized criticality (SOC) (Fig. 1.3). Since then, several models have been proposed to provide a mathematical theory for a class of phenomena that seems to be everywhere in nature.

Other studies [4] has shown that a lot of phenomena we observe in living systems could be traced back to the fact that they seem to calibrate their internal parameters in order to position themselves in the vicinity of critical points; even more interesting is that this tendency to criticality is found at every scale, from proteins to neural networks rather than flocks' collective motion or insects behaviour.

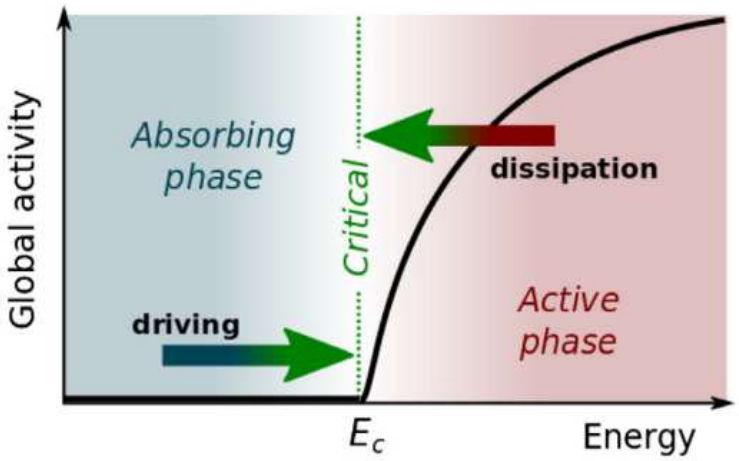

Figure 1.3: The self-organization-to-criticality (SOC) mechanism works by establishing a feedback loop between the dynamics of the activity and that of the control parameter (total accumulated energy, stress, or sand grains) at separated time scales. In particular, the control parameter itself becomes a dynamical variable that operates in opposite ways depending on the system's state: fast dissipation (negative force) dominates while the control parameter lies within the active phase and by slow driving dynamics (positive force) dominates in the absorbing or quiescent phase. This feedback self-organizes the system to the critical point of its second order phase transition if the separation between slow and fast time scales is infinitely large and the dynamics is conservative. Otherwise, the system is just self-organized to the neighborhood of the critical point with excursions around it, i.e., self-organized quasi-criticality [20].

This apparent ubiquity of critical phenomena in living systems could hide the existence of a much more general principle on which the behavior of such systems is based.

1.4 Advantages of Criticality

We discussed several aspects concerning the emergence of criticality in living systems. However, why a living system would want to position itself at criticality? We want, now, to explore what are the possible advantages of criticality that living systems could exploit to enhance their performance.

One important feature that systems at criticality displays is the emergence of large correlation length. Interacting living systems exploit this characteristic of criticality in order to create coordinated and collective behaviour of individual agents across space and time. This has been shown to be relevant in systems where coordination and coherence across extended areas is essential, for example in neural systems [21], flocks of birds [2] and micro-organism colonies [22]. Furthermore, the emergence of very large correlation times and a critical slowing down provide a useful mechanism for the generation of long-lasting and/or slow-decaying memories

at multiple time scales [23].
Moreover, living systems need to perceive and respond to a whole plethora of signal coming both from the environment and from internal interactions between individual; they spontaneously generate complex patterns in order to store highly diverse and detailed pieces of information. The successful construction of these patterns, which extract, summarize, and integrate relevant information [24], provides a crucial competitive advantage, which can eventually make the difference between survival and extinction. The variability of possible spatio-temporal patterns is maximal at criticality, this may allow living systems to exhibit a large repertoire of dynamical responses, optimal transmission and storage of information and high sensitivity to environmental changes ([23], [25], [26]).
Another remarkable feature of living systems is their extraordinary "computational power". It was conjectured long ago that this property could actually be the fingerprint of collective behaviour, emerging out of large number of simple components coming together. First suggested by Turing [27] and Ashby [28] and then further developed in the context of machine learning, networked systems operating at criticality could manifest high computational power. Being at the border between an ordered an a disordered phase constitutes an excellent compromise between between information storage and information transmission, two key ingredients for universal computing machines. Other studies have corroborated that the overall transmission of information between units in a network, as measured by diverse indicators, is maximal if the underlying dynamical process is critical ([29] [30] [31] [32]).

2

Framework for Criticality in Living Systems

We want now to present a framework [13] for understanding how self-tuning to criticality can arise in living systems. Unlike models of self-organized criticality (Section 1.3) in which some inanimate systems are found to become critical in a mechanistic way, we will focus on a more general adaptive or evolutionary mechanisms, specific to biological systems. It is interesting to think that the drive to criticality could actually arise from functional advantages of being in the vicinity of a critical point.

Exploiting general ideas from statistical mechanics and information theory, we want to introduce a quantitative framework showing that self-tuning to criticality is a convenient strategy adopted by living system in order to effectively deal with the complex external world or the internal interactions within individuals. Accordingly, if an individual best model the signals it receives, it will have a better chance of surviving.

To provide some further intuition, let us consider these individuals as having a gene (or neural) regulatory network that represents the internal configuration with which they can respond to external signals by modifying the expression of their genes (neurons). The environment can thus be described as one or more sources of signals that will be perceived and processed by an individual, or one can consider the environment as a community of mutually interacting individuals. Without loss of generality, we assume the state of these gene network to be controlled by some parameters which completely determines the probability distribution of the individual's internal configurations. Each individual will then attempt to modify its configuration in order to best model the signals coming from environmental sources or from other individuals.

As we shall see, by associating a dynamic that gives a more suitable individual a greater chance of survival, the population will evolve by bringing the parameters that define the internal configurations of individuals close to a critical point.

2.1 Evolutionary Models

Let us consider a community of M individuals which are receiving and elaborating with external signals. Each one of them is characterized by a set of N internal variables that, for simplicity, we assume to take binary values. Therefore, the state of each single individual is completely portrayed by the string $\boldsymbol{s} = (s_1, \ldots, s_N) \in \{0, 1\}^N$. A specific external source could be modeled by a probability distribution P_{ext}, which we assume depending on a set of parameters $\boldsymbol{x} = (x_1, x_2, \ldots x_d)$. In order to best understand and interpret the source, an individual will therefore have to modify its internal configuration in order to approximate the P_{ext} distribution. This is achieved by changing its internal state, contained in a second probability distribution function, P_{int}, specified by a different set of parameter $\boldsymbol{y} = (y_1, y_2, \ldots y_d)$ aimed at capturing the essential features of P_{ext} in the most efficient way. We will denote the external source and its internal representation by $P_{ext}(\boldsymbol{s}|\boldsymbol{x})$ and $P_{int}(\boldsymbol{s}|\boldsymbol{y})$ respectively.

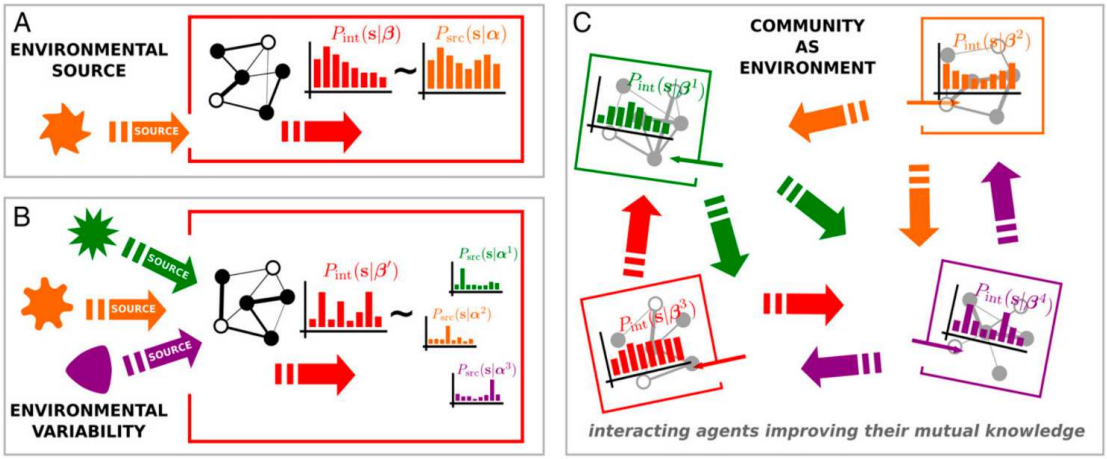

Figure 2.1: Living systems interacting with the environment. In panel A the biological systems cope with the external source by approximating its internal representation $P_{int}(s|y)$ to the environmental source. In this case, $P_{src}(s|x)$ is the best configuration of the variables $\boldsymbol{s}$ in order to efficiently deal with the environment. In panel B, the environment consists of multiple sources and the individual's internal configuration must adapt to all of them. In panel C, the environment consists of the other individuals in the population, each of them is as source $P_{src,i}$ for the others [13].

For the purposes of this dissertation, we will discuss only the case in which the environment

consists of the other individuals in the population, hence individuals try to imitate as much as possible the state of each other. Moreover, let us emphasize that the framework introduced consists in a rather sketched idealization of specific biological systems, which aims at generality rather than specificity. However, to get a better grasp on the usefulness of this framework, one could think of processes that require (or benefit from) a collective response at the community level, e.g. community of bacteria in which individuals are sensitive and responsive to each other and reconfigure their internal state in order to behave similarly to others.

2.1.1 Mathematical Tools

Before proceeding we briefly recall two basic concepts of information theory: the Kullback-Leibler divergence and the Fisher information.

The Kullaback-Leibler (KL) divergence allows for quantifying the difference between two probability distributions. For instance, given the parameter sets $\boldsymbol{x}$ and $\boldsymbol{y}$ characterizing two probability distribution, the KL divergence from the second distribution to the first is defined as

$$D_{KL}(\boldsymbol{x},\boldsymbol{y}) \coloneqq D(P(\cdot|\boldsymbol{x}),P(\cdot|\boldsymbol{y})) = \left\langle \log \frac{P(\cdot|\boldsymbol{x})}{P(\cdot|\boldsymbol{y})} \right\rangle_{\boldsymbol{x}} \tag{2.1}$$

where the average $\langle\cdot\rangle_{\boldsymbol{x}}$ is taken over $P(\cdot|\boldsymbol{x})$. Eq. 2.1 measures the deficit of information when $P(\boldsymbol{s}|\boldsymbol{y})$ is used to approximate $P(\boldsymbol{s}|\boldsymbol{x})$. It is essential to notice that the KL divergence constitutes a pseudo-distance, as it does not obey the triangle inequality, and is not symmetric as in general $D_{KL}(\boldsymbol{x},\boldsymbol{y}) \neq D_{KL}(\boldsymbol{y},\boldsymbol{x})$, except in the case in which both distribution are identical (in which case the divergence vanishes).

The Fisher Information (FI) is a measure of how distinguishable is a (finite) dataset extracted from a probability distribution from another one obtained with slightly different parameter values. For example, there could be a region in $\boldsymbol{x}$ space in which $P(\boldsymbol{s}|\boldsymbol{x})$ are mostly invariant as we change $\boldsymbol{x}$, while in another regions the distribution could be highly sensitive to parameter changes. The FI is defined as

$$\chi_{\alpha\beta}(\boldsymbol{x}) \coloneqq \left\langle \frac{\partial \log P(\cdot|\boldsymbol{x})}{\partial x_\alpha} \frac{\partial \log P(\cdot|\boldsymbol{x})}{\partial x_\beta} \right\rangle_{\boldsymbol{x}} \tag{2.2}$$

for $\alpha,\beta = 1,\dots,d$. Following the Cramér-Rao inequality, which states that the error made when we estimate $\boldsymbol{x}$ from one state $\boldsymbol{s}$ is, on average, greater than (or at least equal to) the inverse

of the Fisher information, if χ happens to diverge at some point, it is possible to specify the associated parameters with maximal precision. It is not surprising that the FI exhibits a peak at critical points.
Indeed, without loss of generality, we can parametrize the internal probability distribution of individuals as:

$$P(\boldsymbol{s}|\boldsymbol{x}) = \frac{\exp\{-\boldsymbol{x}\cdot\boldsymbol{\phi}(\boldsymbol{s})\}}{\sum_{\boldsymbol{s}'}\exp\{-\boldsymbol{x}\cdot\boldsymbol{\phi}(\boldsymbol{s}')\}} \tag{2.3}$$

where $\boldsymbol{\phi} = (\phi_1, \phi_2, \dots)$ are the functions of the internal configuration and $\boldsymbol{x}\cdot\boldsymbol{\phi} = \sum_\alpha x_\alpha\phi_\alpha$. In particular, if $\phi_1(s) = \sum_{i<j}^N s_i s_j/N$ the internal state of each individual corresponds to a mean-field Ising model at some temperature. With this parametrization, the Fisher information is the generalized susceptibility in the statistical mechanics terminology

$$\chi_{\alpha\beta}(\boldsymbol{x}) = -\frac{\partial\langle\phi_\alpha\rangle_{\boldsymbol{x}}}{\partial x_\beta} = \langle\phi_\alpha\phi_\beta\rangle_{\boldsymbol{x}} - \langle\phi_\alpha\rangle_{\boldsymbol{x}}\langle\phi_\beta\rangle_{\boldsymbol{x}} \tag{2.4}$$

which measures the response of the system to parameter variations and is well known to peak at critical points.

2.1.2 Co-evolutionary Model

The Coevolutionary model consists of a community of M individuals aiming at having an internal distribution as similar as possible to the other, as to say that the environment is made up of the other $M-1$ individuals of the community. The Kullback-Leibler divergence of an individual with respect to the others quantifies the individual's understanding of the environment, i.e each individual aim at optimizing the information deficit they have from the rest of the community. Each individual agent is characterized by an internal state (probability distribution function) parametrized as in Eq. 2.3. All individuals are identical in principle, but they may differ in their parameter values.
The dynamics proceeded by randomly selecting at each time step a pair of agents i and j; since the KL in not symmetric, one of the two agents will have a larger fitness, which translates in a higher probability of generating a progeny, due to its informational advantage. On the other hand, the less fit agent is more likely to die and be removed from the community, while the fittest one generates an offspring that inherits its parameter values, with some small mutation. This process is then iterated in time, defining a genetic algorithm. After a sufficient amount time the output of this dynamics turns out to be that the community of agents evolve to have intrinsic parameters located around the corresponding critical point.

It is made the assumption that the fitness just mentioned is proportional to a decreasing function of the KL divergence between the internal distribution of agent i, $P_i(\boldsymbol{s}|\boldsymbol{x})$, and the one of agent j, $P_j(\boldsymbol{s}|\boldsymbol{y})$; namely it is made the assumption that an individual is the fittest if it is able to understand the surrounding environment better than others, i.e. if it makes a minimal error in approximating the distribution of other individuals with its own internal distribution. Given this assumption, the relative fitness of individual i, whose internal distribution depends on $\boldsymbol{x}$, with respect to individual j, whose internal distribution depends on $\boldsymbol{y}$, is defined as

$$f_i^{(j)} := 1 - \frac{D_{KL}(\boldsymbol{y}|\boldsymbol{x})}{D_{KL}(\boldsymbol{x}|\boldsymbol{y}) + D_{KL}(\boldsymbol{y}|\boldsymbol{x})} \tag{2.5}$$

and similarly for the opposite case, $f_j^{(i)}$. Indeed, reviewing Eq. 2.5, it is easy to see that for $D_{KL}(\boldsymbol{y}|\boldsymbol{x}) < D_{KL}(\boldsymbol{x}|\boldsymbol{y})$ - which, by definition, means that i imitates j better than vice versa - one finds $f_i^{(j)} > f_j^{(i)}$, hence that i is the fittest.
As a remark, it is worth pointing out that even though community in which each individual is characterized by the same parameter $\boldsymbol{x}$ seems to be maximally adapted - since the KL divergence goes to zero for $\boldsymbol{x} = \boldsymbol{y}$ and each individual would then be able to represent the group without any loss of information - it is not a stable solution. Indeed, if the two parameters are not identical but close, the difference between their respective KL divergences from each to the other is (see Appendix A)

$$D_{KL}(x + \delta x|x) - D_{KL}(x|x + \delta x) \simeq \frac{1}{6}\nabla\chi(x)\delta x^3 \tag{2.6}$$

This implies that the individual whose parameters correspond to the state with larger χ has a smaller KL divergence and, hence, is fitter. However, as said in Sec. 2.1.1, χ peaks at the critical point, and thus for a family of individuals with similar parameters, the fittest possible agent sits exactly at criticality.

2.1.3 Generalized Model

We now want to generalise the dynamics described in the previous section by introducing into the model a new parameter ν that will be called "strategy". With the introduction of this new parameter we want to study the dynamics of individuals who give some weight to both their own loss of information and that of others, to a greater or lesser extent. In order to achieve this, we use the parameter ν to define a new (pseudo-) distance as a function of the KL divergence,

namely the distance of i from j is

$$D^{\nu_i}(\boldsymbol{y}|\boldsymbol{x}) \coloneqq (1-\nu_i)D_{KL}(\boldsymbol{y}|\boldsymbol{x}) + \nu_i D_{KL}(\boldsymbol{x}|\boldsymbol{y}) \tag{2.7}$$

where $\boldsymbol{x}$ and $\boldsymbol{y}$ are the parameters on which the internal distribution of i and j, respectively, depend and $\nu_i \in [-1/2, 1/2]$ is the strategy of individual i. Conversely, this leads to a slightly modified version of the fitness, which takes into account also the strategies of the two individuals, that is

$$f_i^{(j)} \coloneqq 1 - \frac{D^{\nu_i}(\boldsymbol{y}|\boldsymbol{x})}{D^{\nu_j}(\boldsymbol{x}|\boldsymbol{y}) + D^{\nu_i}(\boldsymbol{y}|\boldsymbol{x})} \tag{2.8}$$

In order to better understand the meaning of D^{ν} it may be useful to exploit some key values of ν.
For instance, the most trivial value is $\nu = 0$, since it gives back the usual KL divergence

$$D^{\nu=0}(\boldsymbol{y}|\boldsymbol{x}) = D_{KL}(\boldsymbol{y}|\boldsymbol{x}) \coloneqq D^{comp}(\boldsymbol{y}|\boldsymbol{x}). \tag{2.9}$$

Individuals which adopt this strategy will be called **Competitors** since they behave as if they are trying to compete with each others by trying to minimize their loss of information.
Another interesting case is for $\nu = 1/2$ which leads to a symmetrized anologous of the KL divergence, i.e. the Jensen-Shannon (JS) divergence [33]

$$D^{\nu=1/2}(\boldsymbol{y}|\boldsymbol{x}) = \frac{D_{KL}(\boldsymbol{y}|\boldsymbol{x}) + D_{KL}(\boldsymbol{x}|\boldsymbol{y})}{2} \coloneqq D^{neutr}(\boldsymbol{y}|\boldsymbol{x}). \tag{2.10}$$

Individuals which adopt this strategy will be called **Neutrals** since they try to minimize both their and others' loss of information. Moreover, following from Eq. 2.8, two neutral agents will always have relative fitnesses of $1/2$, meaning neither of them prevails over the other.
Lastly, for $\nu = -1/2$ the new generalized distance takes the following form:

$$D^{\nu=-1/2}(\boldsymbol{y}|\boldsymbol{x}) = \frac{3D_{KL}(\boldsymbol{y}|\boldsymbol{x}) - D_{KL}(\boldsymbol{x}|\boldsymbol{y})}{2} \coloneqq D^{aggr}(\boldsymbol{y}|\boldsymbol{x}). \tag{2.11}$$

Individuals which adopt this strategy will be called **Aggressive Competitors** since they try to strongly minimize their loss of information, while maximizing others'.
With this generalized model we will try to provide answers to some questions that arise from a game-theory perspective: what is the best strategy for individuals: to be aggressive, to compete,

or just to be neutral? What occurs if we take the optimal strategy for any specific case and introduce a small amount of individuals with different strategies? Is the previous optimal strategy still stable? What happens if we introduce mutations in the strategy?

2.2 Evolutionary Stability

In evolutionary models selection happens because the fitness of an individual is simultaneously influenced by its own strategy, the strategies of others, and other features of the environment. Maynard Smith & Price (1973) [34] considered the fate of a rare mutant or invader playing against some resident population. For evolutionary stability, they suggest *"a strategy such that, if most of the members of a population adopt it, there is no 'mutant' strategy that would give higher reproductive fitness"*.

Resistance to invasion, however, is a static concept. It guarantees that a population monomorphic for an invasion resistant strategy can maintain its position against a rare invader, but it says nothing about what would happen if the population starts at a nearby point. An additional concept, known as convergence stability, is needed to fully characterize the evolutionary stability of strategies. When talking about convergent stable strategies, we refer to strategies to which the system returns after any perturbation that is small enough.

In game theory, the key aspect is examining the fitness of a rare mutant, ν', playing against the strategy field created by a monomorphic population for ν. An Evolutionarily Stable Strategy (ESS) is one that is its own best response. At an ESS an individual maximizes its fitness by playing the same strategy as the population, which makes an ESS resistant to invasion by rare alternative strategies. Adaptive dynamics extends the static nature of game theory by exploring the dynamic processes that lead a population to evolve toward an ESS. Surprisingly, evolution can lead to fitness minima as well as maxima being evolutionary repellors. Adaptive dynamics highlights the importance of convergence stability (being an evolutionary attractor).

These two types of stability are completely independent from each other, conversely a stationary strategy ν^* may exhibit one of four possible outocomes (McGill & Brown 2007 [35]): (1) resistant to invasion and convergent stable, (2) resistant to invasion and not convergent stable, (3) invadable and convergent stable, and (4) invadable and not convergent stable.

- **ESS**: Outcome (1) is defined as Evolutionary Stable Startegy (ESS). This means the ESS is an uninvadable fitness maximum and convergent stable.
- **Branching point**: The term branching point describes outcome (3) where a strategy is both a fitness minimum and convergent stable. Populations may evolve to these branch-

ing points and then under the right conditions diverge into two separate populations or species with distinct strategies.

- **Repelling points**: Outcomes (2) and (4) are not convergent stable. Evolution will not move strategies to these repelling points.

If we want to mathematically formalise these concepts we need to start from the invasion fitness function $f(\nu', \nu)$ describing the long-term per capita growth rate of a rare mutant type ν' in a resident population that is monomorphic for trait value ν. The adaptive dynamics of the trait ν is then given as a gradient dynamics of the invasion fitness function and described by the canonical equation [36]

$$\dot{\nu} = \left.\frac{\partial f(\nu', \nu)}{\partial \nu'}\right|_{\nu'=\nu} \tag{2.12}$$

The partial derivative with respect to the mutant trait is evaluated at the resident trait. Equilibrium points of the adaptive dynamics are then given as points ν^* in phenotype space at which the selection gradient vanishes, i.e., points satisfying

$$\left.\frac{\partial f(\nu', \nu^*)}{\partial \nu'}\right|_{\nu'=\nu^*} = 0 \tag{2.13}$$

The condition for convergence stability of the singular point, i.e., for local stability of an equilibrium of the dynamical system, is given by

$$\frac{\mathrm{d}}{\mathrm{d}\nu}\left[\left.\frac{\partial f(\nu', \nu)}{\partial \nu'}\right|_{\nu'=\nu}\right]\Bigg|_{\nu=\nu^*} = \left.\frac{\partial^2 f(\nu', \nu)}{\partial \nu \partial \nu'}\right|_{\nu'=\nu=\nu^*} + \left.\frac{\partial^2 f(\nu', \nu)}{\partial \nu'^2}\right|_{\nu'=\nu=\nu^*} < 0 \tag{2.14}$$

Similarly, the condition for resistance to invasions of a singular point translates into the fact that the invasion fitness function $f(\nu', \nu^*)$ has, as a function of ν', a maximum at ν^*, hence

$$\left.\frac{\partial^2 f(\nu', \nu)}{\partial \nu'^2}\right|_{\nu'=\nu=\nu^*} < 0, \tag{2.15}$$

for in that case no mutant trait in the vicinity of the singular point has a higher growth rate than the singular trait value itself.

3

Individual Based Model and Results

3.1 Computational Approach

We start by describing the core of the computational approach - based on the Coevolutionary model (Sec. 2.1.2) and its generalised version (Sec. 2.1.3) - used to perform numerical simulations of a community of individuals.
The k^{th} agent of the community is described by a probability distribution

$$P(\boldsymbol{s}|\boldsymbol{x}^k) \propto \exp\{-H_{int}(\boldsymbol{s}|\boldsymbol{x}^k)\}, \tag{3.1}$$

with $H_{int}(\boldsymbol{s}|\boldsymbol{x}^k) = \sum_\alpha x_\alpha^k \phi_\alpha(\boldsymbol{s})$, depending on parameters $\boldsymbol{x}^k$. Starting with an ensemble of M agents whose internal parameters are extracted from an arbitrary distribution, $p(\boldsymbol{x})$, two individuals, i and j, are randomly selected at each time step. Their relative fitnesses are computed following Eq. 2.5 when dealing with the standard Coevolutionary model or Eq. 2.8 for the generalized version of it. One of the two individuals - selected with probability equal to its relative fitness - creates an offspring, while the other one is removed from the community.
The offspring inherits its parameters from its ancestor (with probability $1-\delta$) or mutates with a probability δ, modifying its parameters from $\boldsymbol{x}$ to $\boldsymbol{x} \to \boldsymbol{x} + \boldsymbol{\xi}$, where $\boldsymbol{\xi}$ is a multivariate Gaussian random vector, with uncorrelated components, zero mean, and deviation $\boldsymbol{\sigma}$. Indeed, in general, a genetic algorithm is characterised by two elements: a mechanism of mutation that generates varieties in the population and a selection mechanism which favours some varieties

over others.

Regarding the strategy adopted by individuals in the generalised model, we will be exploring two scenarios: one in which the strategy is fixed, meaning that the offspring will inherit the same strategy of its ancestor and one in which we allow strategy to mutate during the dynamics from ν to $\nu \to \nu + \xi$, where ξ is a Gaussian random variable with zero mean and deviation σ_ν.

Time is, then, updated to $t \to t + dt$, another couple of individuals i' and j' is picked, and the process is iterated.

Defined a systematical algorithm, we can now move on to the choice of a parametrization for the individuals' internal distribution. In particular, we look for a parametrization that would allow us to quickly identify whether or not the system is in a critical regime. A very simple, yet with a very interesting phenomenology, corresponds to the (zero-field) Ising mean-field model parametrization

$$P(\boldsymbol{s}|x) \propto \exp\left\{ x \sum_{i<j}^{N} \frac{s_i s_j}{N} \right\}. \tag{3.2}$$

which has the advantage of having just only one free parameter $\boldsymbol{x} = x$ (usually interpreted as the inverse temperature). We could further simplify the parametrization by assuming that individuals could only take two states, *Up* and *Down*, therefore having, respectively, the following probability distributions

$$P_{up}(x) = \frac{1 + \tanh ax}{2}, \qquad P_{down}(x) = \frac{1 - \tanh ax}{2} \tag{3.3}$$

where a is an arbitrary parameter purposely added to control the sharpness of the Fisher Information (see Fig. 3.1) which, in this parametrization, is

$$\chi(x) = \frac{a^2}{\cosh^2 ax} \tag{3.4}$$

and has a peak at $x^* = 0$.

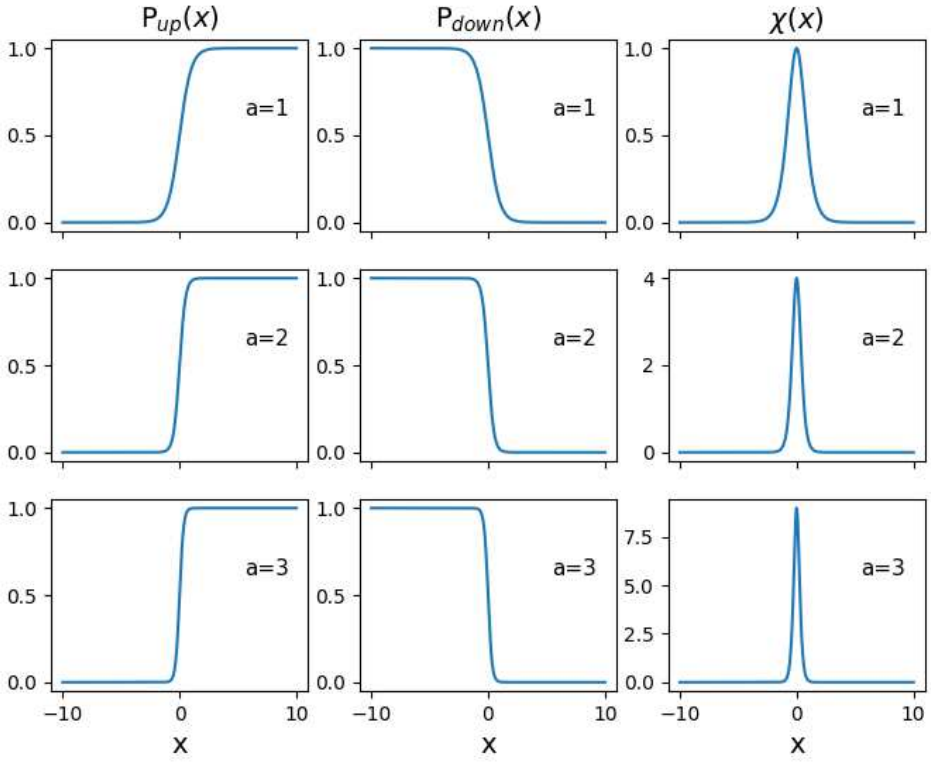

Figure 3.1: Plot of the two internal distributions, $P_{up}(x)$ (**left**) and $P_{down}(x)$ (**middle**), and the F.I., $\chi(x)$ (**right**), associated to the parametrization used for different values of the sharpening parameter a. Higher values of the parameter a translates in a sharper peak at $x^* = 0$ of the Fisher Information.

3.2 Simulations Results

As a first step, we want to reproduce the results obtained by [13] for the parametrization introduced. We considered a population of M = 1000 individuals (all competitors) characterised by an internal distribution controlled by the parameter x at the beginning selected from a random uniform distribution over $[0.5, 1.5)$, far from the critical point. At each time step two individuals were selected at random and made to clash. One of the two individuals is then removed with a probability proportional to the loss of information that one has in approximating the distribution of the other. The removed individual is then replaced with another individual with the parameters of the winner. In order for variety to be generated, the parameters of the "new" individual undergo a mutation process characterized by a mutation rate δ and a Gaussian noise with zero mean and standard deviation σ. In this setting, the population converges

rapidly (see Fig. 3.2) to an equilibrium parameter $x_c = 0$ which corresponds to the peak of the generalised susceptibility of this system (i.e, to a critical point).

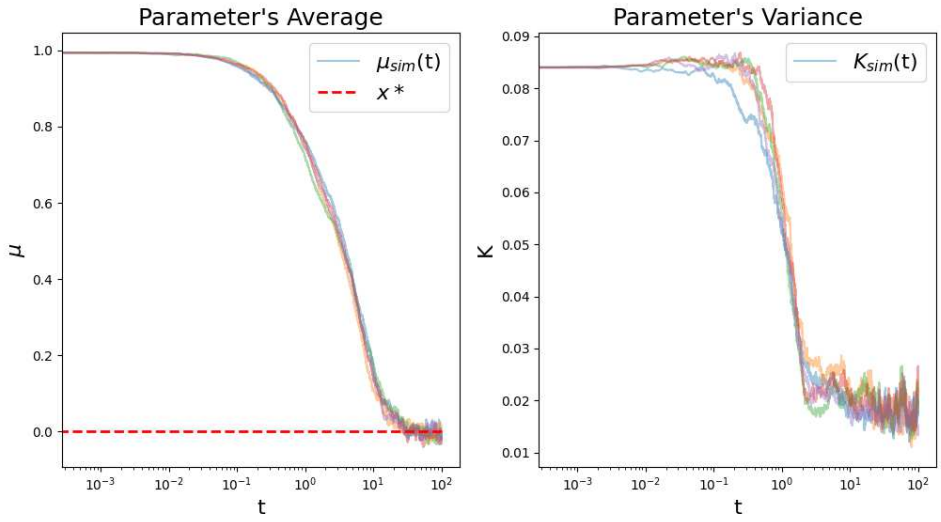

Figure 3.2: Dynamics of the parameter's average μ (left) and parameter's variance K (right) in a population of $M = 1000$ individuals (all **competitors**) for a period of time $t_f = 100$ and time-step $dt = 5e - 4$. The offspring generated at each time-step mutates with a rate $\delta = 0.7$ and Gaussian noise with zero mean and standard deviation $\sigma = 0.05$. Each line represent a different run of the dynamics with the same initial conditions.

3.2.1 Fixed Strategy

The new generalised definition of fitness (Eq. 2.8) let us explore the role of the strategy adopted by individuals. We first simulate a system that has the same characteristics as the one described above, but in which all individuals are neutral (i.e. $\nu = 1/2$).
It is evident from the computational simulation (Fig. 3.3) that, while the competition attracts the population towards the critical point, the evolution over time of neutral agents is purely random (*random walk*). Indeed, the relative fitnesses of two neutral individuals is completely independent of their parameters and, specifically, is always identically equal to $1/2$. Consequently, being "equally fit" in the process of mutual/collective understanding, one of the two individuals is selected at random and the dynamic does not lead to any critical point.

The other extremal case, i.e. $\nu = -1/2$ or as we've named it "aggressive competition", shows similar features to the competitive ($\nu = 0$) case; a population of individuals in which all of

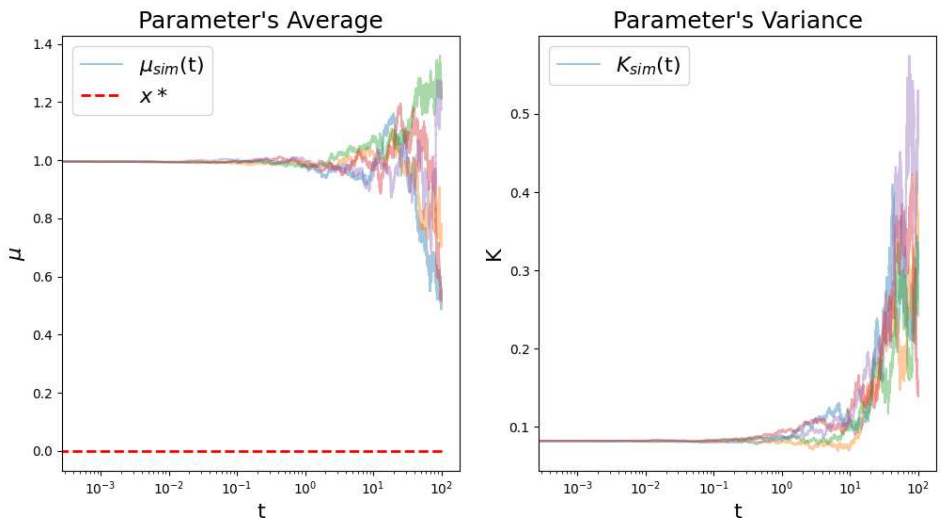

Figure 3.3: Dynamics of the parameter's average μ (left) and parameter's variance K (right) in a population of $M = 1000$ individuals (all **neutrals**) for a period of time $t_f = 100$ and time-step $dt = 5e - 4$. The offspring generated at each time-step mutates with a rate $\delta = 0.7$ and Gaussian noise with zero mean and standard deviation $\sigma = 0.05$. Each line represent a different run of the dynamics with the same initial conditions.

them adopt an aggressive competition strategy is attracted towards a critical point corresponding to the peak of the generalised susceptibility of the system. The only difference that emerges between this two strategy (competition and aggressive competition), at this level of analysis, is the velocity with which they converge to criticality. A population of aggressively competitive individuals seems to converge faster to criticality than a population of competitive individuals.

In order to better understand the significance of competition (or aggressive competition) as an evolutionary argument, we start by studying a population of neutral agents "infected" by a small fraction of competitive individuals. Since we are interested in understanding the effect of competition on the criticality of the system and not, for the moment, on whether or not of having different types of strategy in the population coexisting at once, we've decide that the offspring inherit the exact strategy of its "parent", hence favouring the optimal strategy to proliferate. Indeed, even though neutral agents outnumber competitive individuals in the population we are considering, we shall assume that competition eventually takes over the whole population in this case, since as showed above competition actually leads the system to criticality.

As a matter of fact, this is exactly what we see in Fig. 3.4. The left panel tells us that the pop-

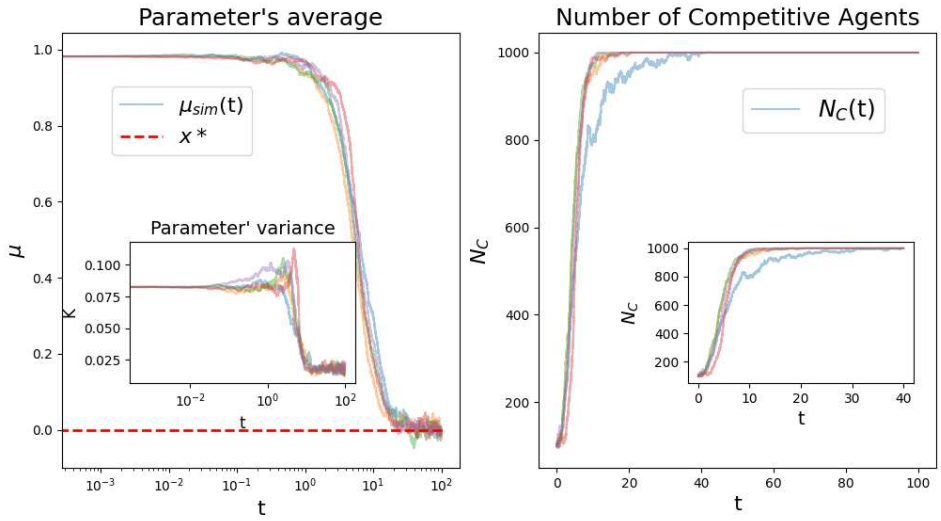

Figure 3.4: Dynamics of the parameter's average μ and variance K (left panel) and of the number of competitive agents N_C (right panel) in a population of $M = 1000$ individuals, 10% of which are competitive and the rest are neutral ones at the start of the dynamics. The system is simulated for a period of time $t_f = 100$ and time-step $dt = 5e - 4$. The offspring generated at each time-step mutates with a rate $\delta = 0.7$, Gaussian noise with zero mean and standard deviation $\sigma = 0.05$ and inherit the strategy parameter ν from its "parent" without any mutation. Each line represent a different run of the dynamics with the same initial conditions.

ulation eventually converges to a critical point even though, as we've seen above, the neutral strategy doesn't lead to convergence. The right panel tells us why this happens: as the system evolves in time competition as a strategy takes over until all individuals adopt it as their strategy. Still, agents inherit the strategy parameter "rigidly" and it was limited to only 3 values up until now. In the next *Section* we let ν span the whole interval it is defined in and let it mutates during the dynamics in order to possibly find an optimal strategy.

3.2.2 Strategy Mutation

Until now, we have considered discrete dynamics for the strategy ν. In order to understand better whether it exist a preferable strategy we let ν change in a continuous way by introducing mutations on the strategy parameter during the evolution of the system. We infer that mutations in the strategy of an individual are less likely then mutations of the internal parameter, hence we assume that the events mutation in the strategy follow a Poisson process, namely

$$P_n(t) = \frac{(\lambda t)^n}{n!} e^{-\lambda t} \tag{3.5}$$

where n is the number of such events (mutation in ν) that occur during a fixed time interval t, and $\lambda \in [0, 1]$ is the rate at which these events occur.
Even though the number of occurrence of events is modeled using a discrete Poisson distribution, the interval of time between consecutive events can be modeled using the Exponential distribution, which is a continuous distribution.
We do this by using the Inverse-CDF technique, in which we literally construct the inverse function of the CDF, and feed it different probability values from a $Uniform(0, 1)$ distribution

$$F_n^{-1}(u) = -\frac{\ln(1-u)}{\lambda} \tag{3.6}$$

After finding the time steps at which we have an event mutation in ν, we run the simulation and at those time steps the offspring inherits a ν form its parent that is $\nu \rightarrow \nu + \delta\nu$, where $\delta\nu \sim \mathcal{N}(0, \sigma_\nu^2)$. Moreover, in order to ensure the value of ν remains in the domain in which we have defined the generalized distance (Eq. 2.7), we impose reflecting boundary condition on ν.

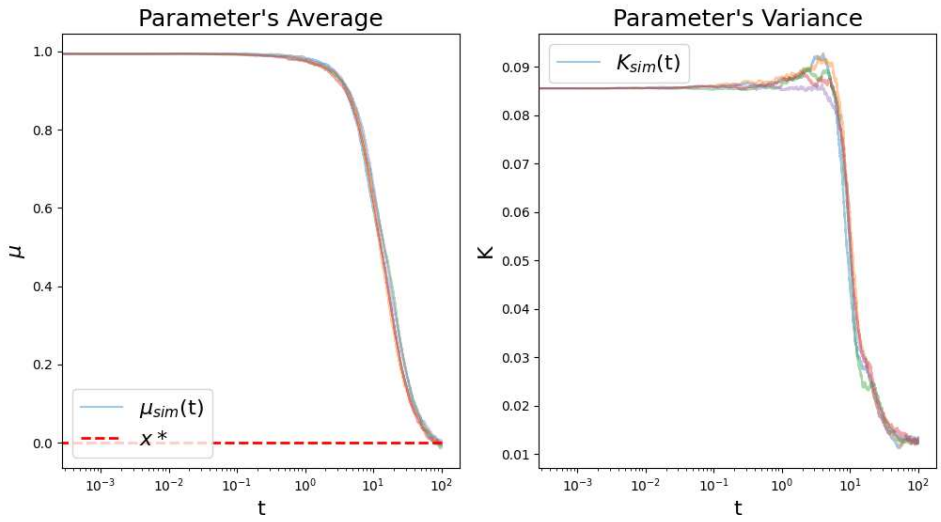

Figure 3.5: Dynamics of the parameter's average μ (left panel) and variance K (right panel) in a population of $M = 5000$ individuals, 10% of which are aggressively competitive and the rest are neutral ones at the start of the dynamics. The system is simulated for a period of time $t_f = 300$ and time-step $dt = 0.001$. The offspring generated at each time-step mutates with a rate $\delta = 0.7$, Gaussian noise with zero mean and standard deviation $\sigma = 0.05$ and inherit the strategy parameter ν from its "parent" with a Poisson mutation process with $\lambda = 0.1$ and $\sigma_\nu = 0.02$. Each line in the left panel represent a different run of the dynamics with the same initial conditions.

We start by simulating a similar system to the one discussed in the previous section with a pop-

ulation composed mainly by neutral individual with a small percentage of aggressive ones. It is important to notice that for these simulations we've increased the number of individuals in the population in order to rule out possible finite size effects in the dynamic of the strategy.
A very small fraction of competitors is sufficient for the population dynamics, with time decreasing as the number of competitors/aggressive competitors increases, to make the system tend towards its critical point again (see Figure 3.5); in fact, if an individual with a more neutral strategy is in a state characterised by a parameter x closer to criticality than an individual with a more competitive strategy with parameter x_0 , i.e. with $x_c < x < x_0$, it will be favoured by the dynamics and this type of clash will in any case attract the population towards a critical point, albeit more slowly than a competitor-competitor clash. Furthermore, in Figure 3.6 it is clear that the population is drawn towards more aggressive strategies. In particular, the final distribution of strategies peaks at $\nu = -1/2$ which is what we've called aggressive competition.

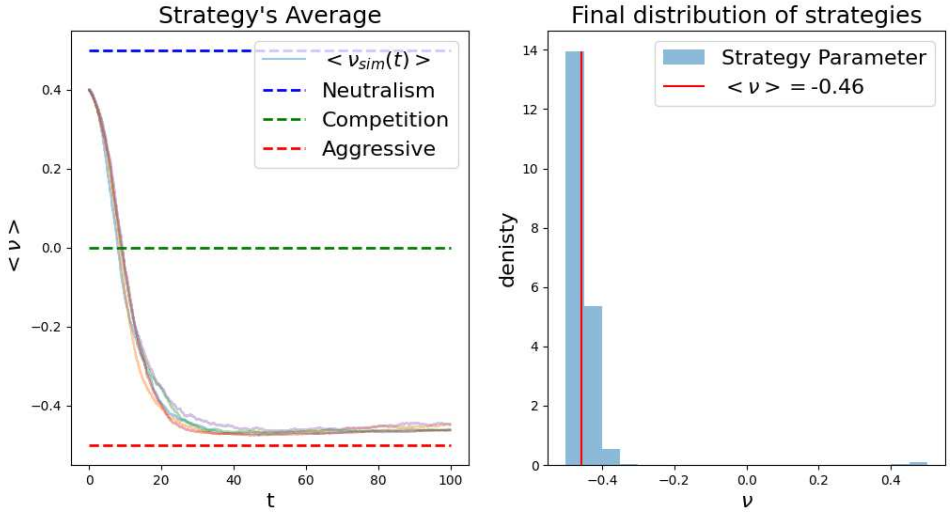

Figure 3.6: Dynamics of the strategy's average μ (left panel) and the final distribution of strategies across the population (right panel) in a system with $M = 5000$ individuals, 10% of which are aggressively competitive and the rest are neutral ones at the start of the dynamics. The system is simulated for a period of time $t_f = 100$ and time-step $dt = 5e - 4$. The offspring generated at each time-step mutates with a rate $\delta = 0.7$, Gaussian noise with zero mean and standard deviation $\sigma = 0.05$ and inherit the strategy parameter ν from its "parent" with a Poisson mutation process with $\lambda = 0.1$ and $\sigma_\nu = 0.02$. Each line in the left panel represent a different run of the dynamics with the same initial conditions. The final distribution of strategies is taken form the last 10 time-steps of the dynamics

Even more remarkable are the results for a population started with a uniform distribution of the strategies Fig. 3.7. The dispersion in the distribution of the strategies is a little bit higher than

in the previous case, however we can confidently say that the population is attracted toward a configuration in which individuals play aggressively between each other.

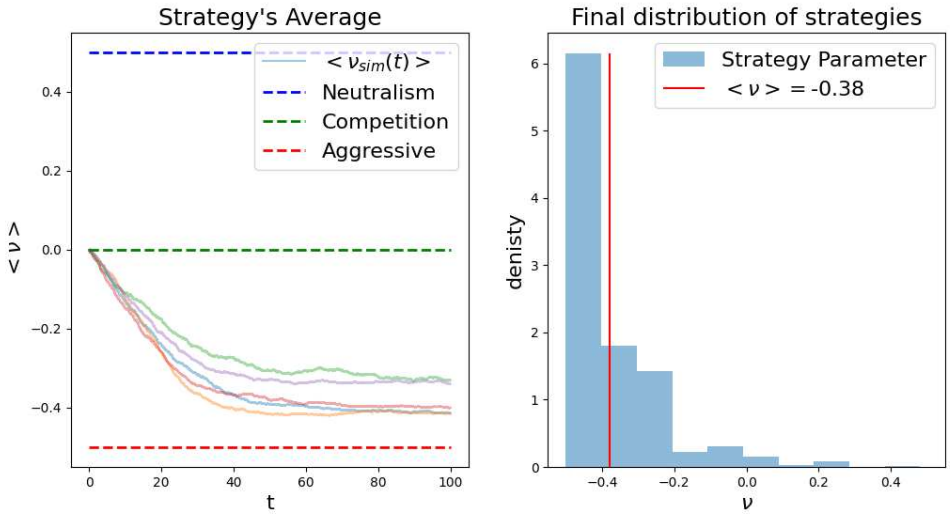

Figure 3.7: Dynamics of the strategy's average μ (left panel) and the final distribution of strategies across the population (right panel) in a system with $M = 5000$ individuals with uniform strategies distribution at the start of the dynamics. The system is simulated for a period of time $t_f = 100$ and time-step $dt = 5e - 4$. The offspring generated at each time-step mutates with a rate $\delta = 0.7$, Gaussian noise with zero mean and standard deviation $\sigma = 0.05$ and inherit the strategy parameter ν from its "parent" with a Poisson mutation process with $\lambda = 0.1$ and $\sigma_\nu = 0.02$. Each line in the left panel represent a different run of the dynamics with the same initial conditions. The final distribution of strategies is taken form the last 10 time-steps of the dynamics

4

Analytical Model and Results

We've now presented mostly computational results, even if some heuristic understanding was also provided. Our first goal now is to construct a version of the individual based model that, while leaving intact the main phenomenology allows for analytical treatment.
Here we discuss both an already known model from the literature as well as an original one, stressing their similitudes and differences. Both models consist of a community of M individuals aiming at having an internal state/distribution as similar as possible to the others, as quantified by their KL divergences to other individuals, i.e. aiming at optimizing the information they have from the rest of the community, i.e. at minimizing its information deficit. In both cases, individual agents are characterized by an internal state (probability distribution function) parametrized as described in the previous *Chapter*. All individuals are identical in principle, but they may differ in their parameter values.

4.1 Heuristic Adaptive Model

This model, introduced by *Hidalgo et. al* [14], is not an evolutionary one, in the sense that agents do not die nor reproduce. Instead it is an adaptive one in which agents slightly change their parameters trying to enhance their fitness.
Each agent i is modelled by its position in parameter space $\boldsymbol{x}^i$. It experiences an adaptive force which is a function of its information-deficit respect to the other agents, plus some stochastic noise and that can be written as the derivative of some (pseudo-) potential, V. In particular,

the adaptive model is defined by means of the set of Langevin equations

$$\dot{\boldsymbol{x}}^i = \frac{1}{M}\sum_{j=1}^{M} \boldsymbol{F}(\boldsymbol{x}^j, \boldsymbol{x}^i) + \sqrt{2T}\boldsymbol{\eta}^i(t), \tag{4.1}$$

for $i = 1, \ldots, M$, where

$$\boldsymbol{F}(\boldsymbol{x}^j, \boldsymbol{x}^i) = -\nabla_{\boldsymbol{x}^i} V(D(\boldsymbol{x}^j, \boldsymbol{x}^i)) \tag{4.2}$$

is the force that an individual agent j produces on an agent i.
The first term on the r.h.s. of Eq. 4.1 is the averaged force acting upon agent i, which points in the direction of the potential gradient. It is important to note that, in general, V is a pseudo-potential and not a true potential, because, due to the asymmetry of the KL divergence, D, the forces in Eq. 4.1 do not obey the potentiality (Schwarz) condition. Still, even in such cases, the force can be defined as the derivative of such a pseudo-potential. The second term in Eq. 4.1 represents a thermal noise where $\sqrt{2T}$ modulates the noise amplitude and $\boldsymbol{\eta}^i$ is a white noise with $\left\langle \eta^i_\alpha(t)\eta^j_\beta(t')\right\rangle = \delta^{ij}\delta_{\alpha\beta}\delta(t-t')$ ($i, j = 1, \ldots M$ and $\alpha, \beta = 1, \ldots, d$).
Lastly, to complete the model definition we need to specify functional form of the pseudo-potential $V(D(\boldsymbol{x}^j, \boldsymbol{x}^i))$. The main constraint we need to impose is that V has to increase monotonically with D (i.e. $V'(D) \geq 0\, \forall D \geq 0$) in order to guarantee that the dynamical process, which converges to minima of V , leads also to minimal values of the KL divergence. In this way, at each time step, each agent i changes its parameters, $\boldsymbol{x}^i$, in the direction of the gradient of V, with some added stochasticity. Here we restrict our analysis to the case of a convex potential $V''(D) > 0$ (see *Hidalgo et. al* [14] Appendix A for more insights).
Moreover, to account for all the different strategies presented in *Section* 2.1.3, we can redefine the potential (and conversely the forces) between individuals i and j as a linear combination of their respective information-deficits. We will consider two types of strategy dependent potentials: the one used in [14] and one with a definition similar to the one we gave for the generalized distance 2.7, which are respectively

$$V^\nu_{(1)}(\boldsymbol{x}^j, \boldsymbol{x}^i) = V(D(\boldsymbol{x}^j, \boldsymbol{x}^i)) + (2\nu - 1)V(D(\boldsymbol{x}^i, \boldsymbol{x}^j)) \tag{4.3}$$

$$V^\nu_{(2)}(\boldsymbol{x}^j, \boldsymbol{x}^i) = (1-\nu)V(D(\boldsymbol{x}^j, \boldsymbol{x}^i)) + \nu V(D(\boldsymbol{x}^i, \boldsymbol{x}^j)) \tag{4.4}$$

where, for the first, the parameter $\nu \in [0, 1]$ tunes the interaction from aggressive competition ($\nu = 0$) to neutralism ($\nu = 1$), including the intermediate competitive case ($\nu = 1/2$). The

strategy parameter ν could be seen as a "symmetry coefficient" as, $V_{(1)}^{\nu=0}$ and $V_{(1)}^{\nu=1}$ are anti-symmetric and symmetric functions, respectively, under the exchange $i \leftrightarrow j$. For the second definition the parameter $\nu \in [-1/2, 1/2]$ tunes the interaction from aggressive competition ($\nu = -1/2$) to neutralism ($\nu = 1/2$), including the intermediate competitive case ($\nu = 0$). In this case the strategy parameter ν weight the respective information-deficits of i and j.
Having specified the shape of V and thus the model, the question is: where does the community evolve to as a consequence of this information-based dynamics and does it have similar stationary behaviour as the evolutionary model described the previous *Chapter*? In the next section we present a mathematical approach to compute the attractors of the dynamics in the space of parameters $\boldsymbol{x}$.

4.1.1 Community Dynamics

Retracing the steps followed by *Hidalgo et al.* [14], we begin by analyzing the evolution of the distribution of agents in parameter space, defined as

$$\rho(\boldsymbol{x}, t) = \frac{1}{M} \sum_{i=1}^{M} \delta(\boldsymbol{x}^i(t) - \boldsymbol{x}) \tag{4.5}$$

Following the method proposed by Dean in [37] which allows us to derive an equation for $\partial_t \rho(\boldsymbol{x}, t)$ from Eq. 4.1, we are lead to the following equation for the probability distribution

$$\partial_t \rho(\boldsymbol{x}, t) = -\nabla_{\boldsymbol{x}} \cdot \left(\rho(\boldsymbol{x}, t) \int \mathrm{d}y \, \rho(\boldsymbol{y}, t) \boldsymbol{F}^{\nu}(\boldsymbol{y}, \boldsymbol{x}) \right) + T \nabla^2_{\boldsymbol{x}} \rho(\boldsymbol{x}, t) + \\ + \sqrt{\frac{2T}{N}} \nabla_{\boldsymbol{x}} \cdot \left(\sqrt{\rho(\boldsymbol{x}, t)} \boldsymbol{\xi}(\boldsymbol{x}, t) \right) \tag{4.6}$$

where $\boldsymbol{\xi}(\boldsymbol{x}, t)$ is a new Gaussian noise with zero mean and correlation $\langle \xi_\alpha(\boldsymbol{x}, t) \eta_\beta(\boldsymbol{x}', t') \rangle = \delta_{\alpha\beta} \delta(\boldsymbol{x} - \boldsymbol{x}') \delta(t - t')$ ($i, j = 1, \ldots M$ and $\alpha, \beta = 1, \ldots, d$), interpreted in the Ito's sense. In the limit $N \to \infty$, Eq. 4.6 becomes deterministic, and we find an equation for $\rho(\boldsymbol{x}, t)$, which, roughly speaking, is a sort of non-linear Fokker-Planck equation in which the drift term depends on the distribution ρ itself.
Employing Eq. 4.6 it is possible to derive a set of deterministic equations for the evolution of its moments for $N \to \infty$. The mean $\boldsymbol{\mu}(t) = \int \mathrm{d}\boldsymbol{x} \, \rho(\boldsymbol{x}, t) \boldsymbol{x}$ can be obtained multiplying Eq.

4.6 by $\boldsymbol{x}$ and integrating by parts:

$$\dot{\mu}_\alpha = \int \mathrm{d}\boldsymbol{x}\, \rho(\boldsymbol{x},t) \int \mathrm{d}\boldsymbol{y}\, \rho(\boldsymbol{y},t) F^\nu_\alpha(\boldsymbol{y},\boldsymbol{x}) \tag{4.7}$$

where $\alpha = 1,\ldots,d$. Similarly, for the covariance matrix, defined as $K_{\alpha\beta}(t) = \int \mathrm{d}\boldsymbol{x}\, \rho(\boldsymbol{x},t)(x_\alpha - \mu_\alpha(t))(x_\beta - \mu_\beta(t))$, we find

$$\dot{K}_{\alpha\beta} = 2T\delta_{\alpha\beta} + \sum_{\gamma,\varepsilon=1}^{d} (\delta_{\alpha\gamma}\delta_{\beta\varepsilon} + \delta_{\alpha\varepsilon}\delta_{\beta\gamma}) \int \mathrm{d}\boldsymbol{x}\, \rho(\boldsymbol{x},t)(x_\gamma - \mu_\gamma) \int \mathrm{d}\boldsymbol{y}\, \rho(\boldsymbol{y},t) F^\nu_\varepsilon(\boldsymbol{y},\boldsymbol{x}) \tag{4.8}$$

(for more insights on the derivation of these results see *Appendix* B).
These equations cannot be integrated as the evolution of the mean and covariance matrix still depends on the whole distribution ρ, i.e. they are not a closed set of equations. However, in the next *Section* we present the approximation derived in [14], which allow us to circumvent this difficulty and characterize the evolution of the community by the mean and covariance matrix of the distribution in parameter space.

4.1.2 Explicit Moments Equations

To derive an approximate scheme that give rise to a closed set of explicit equations for the evolution of the mean and covariance matrix of parameters in the community, we first expand $\boldsymbol{F}^\nu(\boldsymbol{y},\boldsymbol{x})$ around $(\boldsymbol{y},\boldsymbol{x}) = (\boldsymbol{\mu}(t),\boldsymbol{\mu}(t))$ in Eqs. 4.7 and 4.8, and integrate over $\boldsymbol{x}$ and $\boldsymbol{y}$; the result is then implicitly given as a function of moments of ρ.
For the purpose of this study, we will consider the potential to be harmonic (i.e. $V(D) = D^2/2$). Keeping only the first contributing terms, we find that for $V^\nu_{(1)}$ given by Eq. 4.3 the explicit moments equations are:

$$\begin{aligned}\dot{\mu}_\varepsilon(t) = {} & (1-\nu)\frac{V''(0)}{4} \sum_{\alpha,\beta,\gamma,\delta=1}^{d} (\chi_{\alpha\varepsilon}(\boldsymbol{\mu})\chi_{\beta\gamma\delta}(\boldsymbol{\mu}) + sym[\alpha,\beta,\gamma,\delta]) \left(K_{\alpha\beta}K_{\gamma\delta} + \frac{K_{\alpha\beta\gamma\delta}}{3} \right) \\ & + (1-2\nu)\frac{V''(0)}{4} \sum_{\alpha,\beta,\gamma,\delta=1}^{d} (\chi_{\alpha\beta}(\boldsymbol{\mu})\chi_{\gamma\delta\varepsilon}(\boldsymbol{\mu}) + sym[\alpha,\beta,\gamma,\delta]) \left(K_{\alpha\beta}K_{\gamma\delta} + \frac{K_{\alpha\beta\gamma\delta}}{3} \right)\end{aligned} \tag{4.9}$$

$$\dot{K}_{\varepsilon\tau}(t) = 2T\delta_{\varepsilon\tau} - \nu V''(0) \sum_{\alpha,\beta,\gamma=1}^{d} (\chi_{\alpha\beta}(\boldsymbol{\mu})\chi_{\gamma\varepsilon}(\boldsymbol{\mu}) + sym[\alpha,\beta,\gamma,\varepsilon]) \left(K_{\alpha\beta}K_{\gamma\tau} + \frac{K_{\alpha\beta\gamma\tau}}{3} \right)$$
$$- \nu V''(0) \sum_{\alpha,\beta,\gamma=1}^{d} (\chi_{\alpha\beta}(\boldsymbol{\mu})\chi_{\gamma\tau}(\boldsymbol{\mu}) + sym[\alpha,\beta,\gamma,\varepsilon]) \left(K_{\alpha\beta}K_{\gamma\varepsilon} + \frac{K_{\alpha\beta\gamma\varepsilon}}{3} \right) \tag{4.10}$$

where $sym[\alpha_1, \ldots, \alpha_p]$ represents the minimal set of terms, obtained via index permutations of its precedent elements, that we have to include to symmetrize the expression under the exchange of indexes $\{\alpha_1, \ldots, \alpha_p\}$ and where $\chi_{\alpha\beta\gamma}(\boldsymbol{\mu}) = \partial_{x_\alpha}\chi_{\beta\gamma}(\boldsymbol{x})|_{\boldsymbol{x}=\boldsymbol{\mu}}$. Equations 4.9 and 4.10 cannot be integrated, as we still need additional equations for the 4-th moment $K_{\alpha\beta\gamma\delta}$. However, we can circumvent this problem by approximating the 4-th moment in terms of the second ones (moment closure). Thus we assume that ρ is approximately Gaussian. Therefore, we simply take $K_{\alpha\beta\gamma\delta} \simeq K_{\alpha\beta}K_{\gamma\delta} + K_{\alpha\gamma}K_{\beta\delta} + K_{\alpha\delta}K_{\beta\gamma}$, obtaining closed equations for the first and second moments. In particular, for the case of just one parameter ($d = 1$) we find:

$$\dot{\mu}(t) = 2(2 - 3\nu)V''(0)\chi(\mu)\partial_\mu\chi(\mu)K^2 \tag{4.11}$$
$$\dot{K}(t) = 2T - 12\nu V''(0)\chi^2(\mu)K^2 \tag{4.12}$$

Equations 4.11 and 4.12 can now be integrated. Indeed *Figures* 4.1, 4.2 and 4.3 show the mean and the variance of the parameter x calculated both by means of the Langevin equation 4.1 (colored lines) and by numerical integration of Eqs. 4.11 - 4.12 (black lines) in the case $d = 1$ with generalized susceptibilty given by Eq. 3.4.
Observe that only for $V_{(1)}^{\nu=1/2}$ - i.e. competitors Fig. 4.1- we get satisfactory results that match the behaviour seen in the co-evolutionary model results (*Chapter* 3). The other two cases, on the other hand, present some problems. For $\nu = 0$ - i.e. aggressive competitors Fig. 4.2 - Eq. 4.12 is no more valid and going to higher order in the expansion of the force $F^\nu(y, x)$ does not resolve the problem. However, at least the results of the simulated Langevin dynamics seem to well match the behaviour we are seeking for. It is not true though for $\nu = 1$ - i.e. neutrals Fig. 4.3 - which gives results in complete contrast with the one obtained in the co-evolutionary model for neutral only agents.

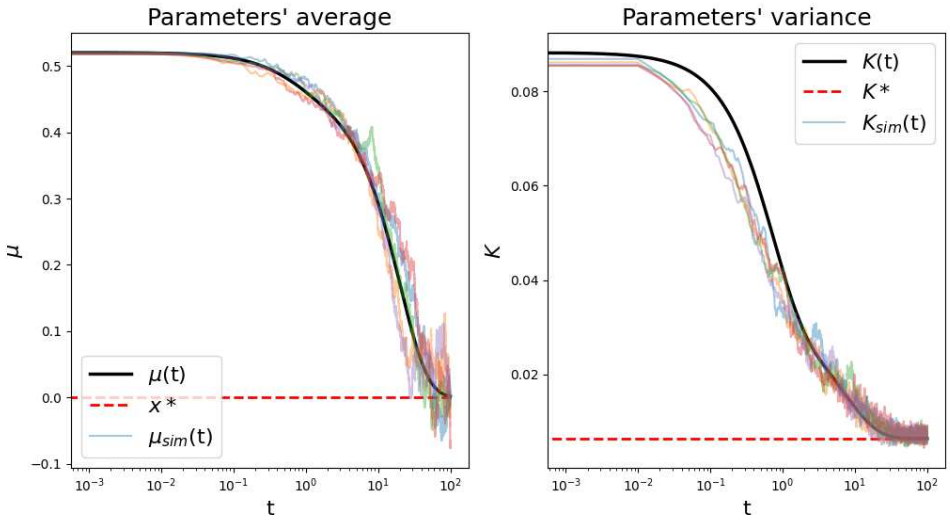

Figure 4.1: Adaptive dynamics of the parameter's average μ (left) and parameter's variance K (right) in a population of $M = 100$ individuals ($\nu = 1/2$ i.e. competitors) for a period of time $t_f = 100$. The colored lines represent the simulated Langevin dynamics obtained from Eq. 4.1, whereas the black solid lines are the numerical integration of the explict moments equations 4.11 and 4.12.

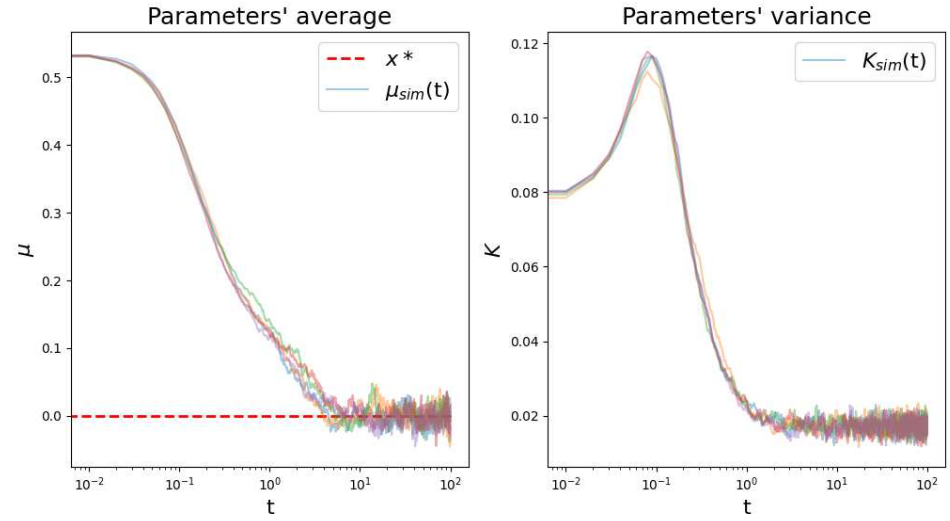

Figure 4.2: Adaptive dynamics of the parameter's average μ (left) and parameter's variance K (right) in a population of $M = 100$ individuals ($\nu = 0$ i.e. aggressive competitors) for a period of time $t_f = 100$. The colored lines represent the simulated Langevin dynamics obtained from Eq. 4.1.

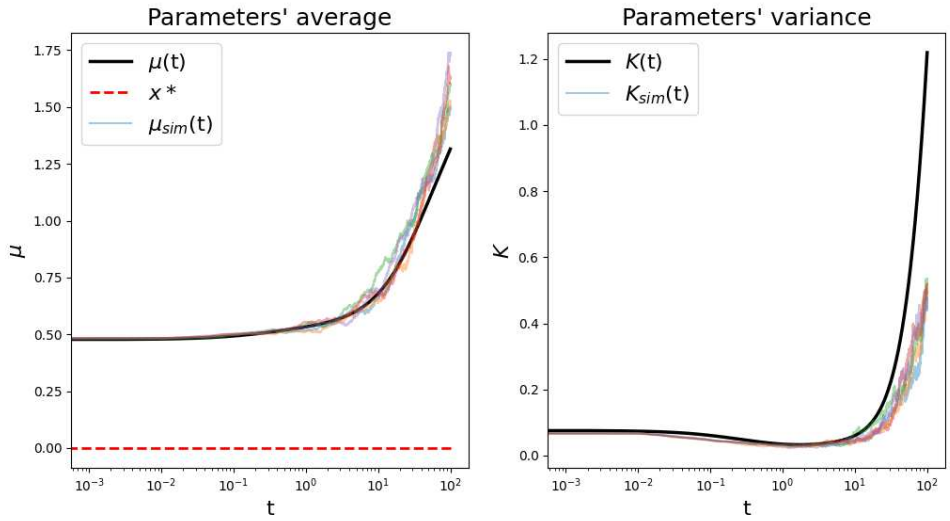

Figure 4.3: Adaptive dynamics of the parameter's average μ (left) and parameter's variance K (right) in a population of $M = 100$ individuals ($\nu = 1$ i.e. neutrals) for a period of time $t_f = 100$. The colored lines represent the simulated Langevin dynamics obtained from Eq. 4.1, whereas the black solid lines are the numerical integration of the explict moments equations 4.11 and 4.12.

Analogously, for $V^{\nu}_{(2)}$ give by Eq. 4.4, we arrive at the following dynamical equations for the mean and the covariance matrix

$$\dot{\mu}_{\varepsilon} = \frac{V''(0)}{8} \sum_{\alpha,\beta,\gamma,\delta=1}^{d} (\chi_{\alpha\beta\gamma}(\boldsymbol{\mu})\chi_{\delta\varepsilon}(\boldsymbol{\mu}) + sym[\alpha,\beta,\gamma,\delta]) \left(K_{\alpha\beta}K_{\gamma\delta} + \frac{K_{\alpha\beta\gamma\delta}}{3} \right)$$
$$- \frac{\nu V''(0)}{4} \sum_{\alpha,\beta,\gamma,\delta=1}^{d} (\chi_{\alpha\beta\gamma}(\boldsymbol{\mu})\chi_{\delta\varepsilon}(\boldsymbol{\mu}) + sym[\alpha,\beta,\gamma,\delta,\varepsilon]) \left(K_{\alpha\beta}K_{\gamma\delta} + \frac{K_{\alpha\beta\gamma\delta}}{3} \right) \tag{4.13}$$

$$\dot{K}_{\varepsilon\tau} = 2T\delta_{\varepsilon\tau} - V''(0) \sum_{\alpha,\beta,\gamma=1}^{d} (\chi_{\alpha\beta}(\boldsymbol{\mu})\chi_{\gamma\varepsilon}(\boldsymbol{\mu}) + sym[\alpha,\beta,\gamma,\varepsilon]) \left(K_{\alpha\beta}K_{\gamma\tau} + \frac{K_{\alpha\beta\gamma\tau}}{3} \right)$$
$$- V''(0) \sum_{\alpha,\beta,\gamma=1}^{d} (\chi_{\alpha\beta}(\boldsymbol{\mu})\chi_{\gamma\tau}(\boldsymbol{\mu}) + sym[\alpha,\beta,\gamma,\tau]) \left(K_{\alpha\beta}K_{\gamma\varepsilon} + \frac{K_{\alpha\beta\gamma\varepsilon}}{3} \right) \tag{4.14}$$

which, for the case of just one parameter ($d = 1$) and using the moment closure approximation

to write 4-th moment in terms of the second ones, become

$$\dot{\mu}(t) = (1 - 5\nu)V''(0)\chi(\mu)\partial_\mu\chi(\mu)K^2 \tag{4.15}$$

$$\dot{K}(t) = 2T - 6V''(0)\chi^2(\mu)K^2 \tag{4.16}$$

Figures 4.4, 4.5 and 4.6 show the mean and the variance of the parameter x calculated both by means of the Langevin equation 4.1 (colored lines) and by numerical integration of Eqs. 4.15 - 4.16 (black lines) in the simplified case of $M = 1$ with generalized susceptibilty given by Eq. 3.4.

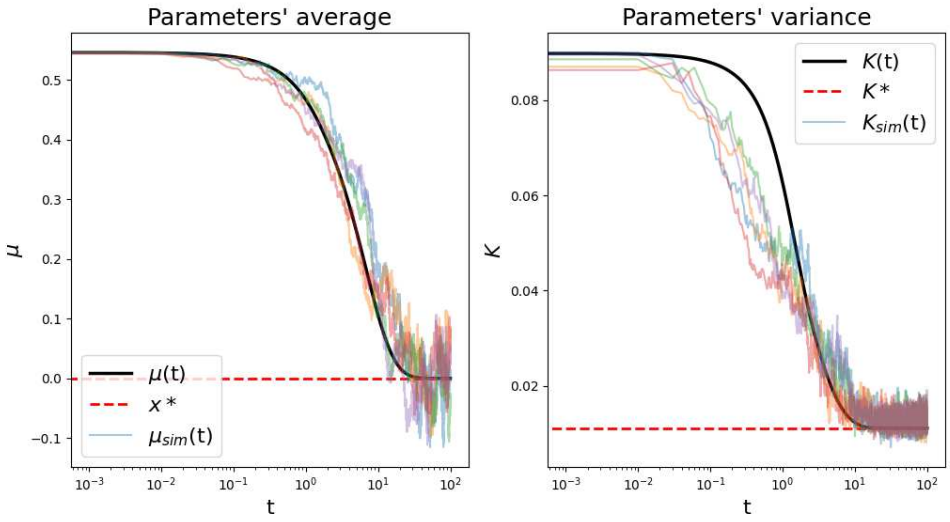

Figure 4.4: Adaptive dynamics of the parameter's average μ (left) and parameter's variance K (right) in a population of $M = 100$ individuals ($\nu = 0$ i.e. competitors) for a period of time $t_f = 100$. The colored lines represent the simulated Langevin dynamics obtained from Eq. 4.1, whereas the black solid lines are the numerical integration of the explict moments equations 4.15 and 4.16.

With this potential we get slightly more satisfactory results than the previous one since the explicit analytical equations work also for the aggressive strategy. However, the problem in the behaviour of the neutral strategy is present also in this case. This may suggest that we cannot consider the forces as the gradient of some arbitrary potential, but a more detailed and well thought definition of the forces is needed.

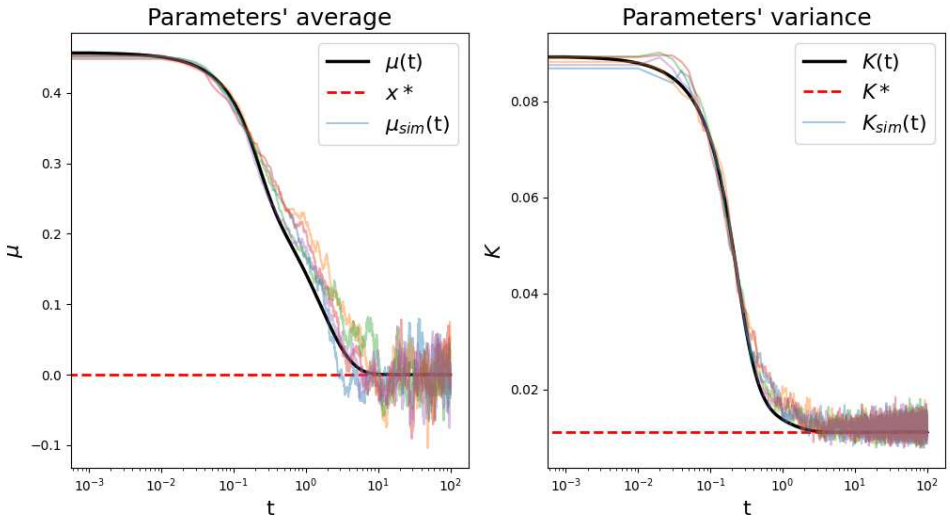

Figure 4.5: Adaptive dynamics of the parameter's average μ (left) and parameter's variance K (right) in a population of $M = 100$ individuals ($\nu = -1/2$ i.e. aggressive competitors) for a period of time $t_f = 100$. The colored lines represent the simulated Langevin dynamics obtained from Eq. 4.1, whereas the black solid lines are the numerical integration of the explict moments equations 4.15 and 4.16..

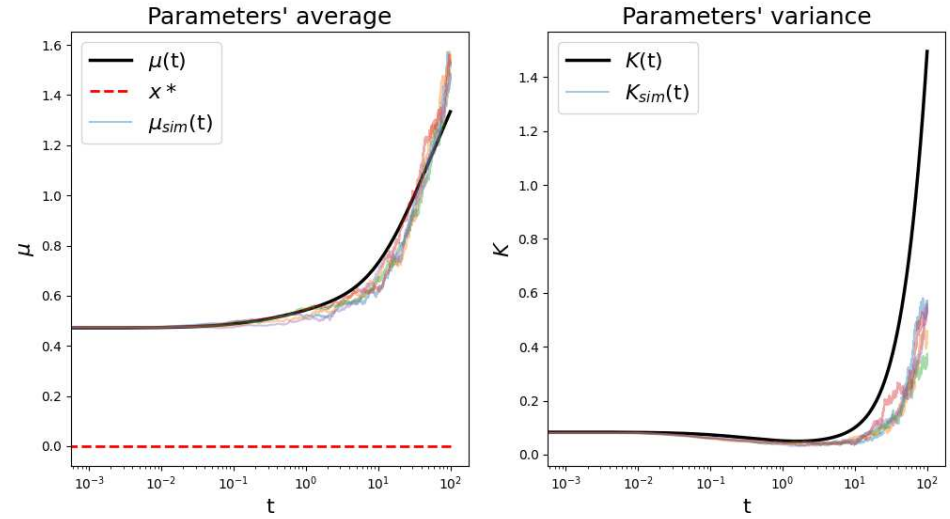

Figure 4.6: Adaptive dynamics of the parameter's average μ (left) and parameter's variance K (right) in a population of $M = 100$ individuals ($\nu = 1/2$ i.e. neutrals) for a period of time $t_f = 100$. The colored lines represent the simulated Langevin dynamics obtained from Eq. 4.1, whereas the black solid lines are the numerical integration of the explict moments equations 4.15 and 4.16.

4.2 Formal Adaptive Model

The adaptive model presented in the previous *Section* is based on the heuristic argument that the forces, acting between individuals of the population, can be represented as the gradient of some arbitrary potential. This argument seems to work fairly fine for competitive strategies, but it fails to predict the behaviour of a population formed by neutral individuals, which makes it incomplete.

We want to give a more comprehensive description of the adaptive dynamics, one that follows a rigorous route. Our starting point for building the analytic description we seek is the general master equation, namely

$$\partial_t \rho(x,t) = \int [W(x|y)\rho(y,t) - W(y|x)\rho(x,t)]\,\mathrm{d}y \tag{4.17}$$

where the transition rates are calculated by following the definition of individual relative fitness (Eq. 2.8), hence

$$W(y|x) = \frac{D_{KL}^{\nu_x}(y|x)}{D_{KL}^{\nu_x}(y|x) + D_{KL}^{\nu_y}(x|y)}, \tag{4.18}$$

Focusing, for now, only on the cases in which the population is formed by individuals with all the same strategy, as to say $\nu_x = \nu_y = \nu$, we can obtain a slightly simplified expression for the transition rates, namely

$$\begin{aligned} W(y|x) &= \frac{D_{KL}^{\nu}(y|x)}{D_{KL}(y|x) + D_{KL}(x|y)} \\ &= \frac{(1-\nu)\tanh ay - \nu \tanh ax}{\tanh ay - \tanh ax} + \frac{(2\nu-1)(\log(\cosh ay) - \log(\cosh ax))}{a(y-x)(\tanh ay - \tanh ax)} \end{aligned} \tag{4.19}$$

Notice how, with this method, we've already solved the problem that we had previously. Indeed, a system formed by only neutral individuals ($\nu = 1/2$) would have transition rates identically equal to $1/2$, hence it would produces simply a random walk dynamics, as we would have expected.

The other cases, however, are not trivial and need some other investigation in order to produce meaningful and useful results. One way of approaching the problem is through the Kramers-Moyal expansion ([38]-[39]) with which we can derive from the master equation (Eq. 4.17) its

associated Fokker-Plank equation, namely

$$\partial_t \rho(x,t) = -\partial_x \left[A_1(x)\rho(x,t) - \frac{1}{2}\partial_x \left(A_2(x)\rho(x,t) \right) \right] \tag{4.20}$$

where $A_1(x)$ and $A_2(x)$ are the coefficient of the first two orders of the Kramers-Moyal expansion of the master equation, calculated as

$$A_k(x) = \int \mathrm{d}y \, (y-x)^k W(y|x). \tag{4.21}$$

The expression of the transition rates Eq. 4.19, however, contains an intricate combination of hyperbolic functions; therefore, if we want to analytically compute the Kramers-Moyal coefficients, we need to introduce an approximation that simplifies the expression of the transition rates.
For instance, assuming that small jumps in the value of internal parameter are favoured, which it mathematically translates into assuming that $\Delta x = y - x \ll 1$, it is possible to re-write the transition rate as a function of $x + \Delta x$ and x and expand around $\Delta x \approx 0$ obtaining an approximation for the transition rate that is much more simple to deal with, namely

$$W(x + \Delta x|x) \simeq \frac{1}{2} + \frac{(2\nu - 1)a}{6} \tanh(ax)\Delta x + \frac{(2\nu - 1)}{12}\chi(x)\Delta x^2 \tag{4.22}$$

where $\chi(x) = a^2/\cosh^2(ax)$ is the generalized susceptibility. It is now straightforward to compute the coefficient of the Kramers-Moyal expansions that happen to be:

$$A_1(x) = \frac{(2\nu - 1)a}{9} dx^3 \tanh(ax) \tag{4.23}$$

$$A_2(x) = \frac{1}{3}dx^3 + \frac{2\nu - 1}{30}dx^5 \chi(x) \tag{4.24}$$

where dx is an arbitrary cut-off in the size of the jumps, $\Delta x \in [-dx, +dx]$.
Having an expression for the drift coefficient, $A_1(x)$, and for the diffusion coefficient, $A_2(x)$, let us also write the Langevin equation associated to the Fokker-Plank equation 4.20, which reads

$$\mathrm{d}x\,(t) = A_1(x)\,\mathrm{d}t + \sqrt{A_2(x)}\,\mathrm{d}\eta\,(t) \tag{4.25}$$

where $\eta(t)$ is the stochastic variable characterised by $\langle \eta(t) \rangle = 0$ and $\langle \eta(t)\eta(t') \rangle = \delta(t - t')$.

Figure 4.7 and 4.8 show the results of the simulated Langevin dynamics obtained with the coefficients of the Kramers-Moyal expansion for the cases $\nu = 0$ and $\nu = -1/2$, respectively, compared with the results of the individual based model.

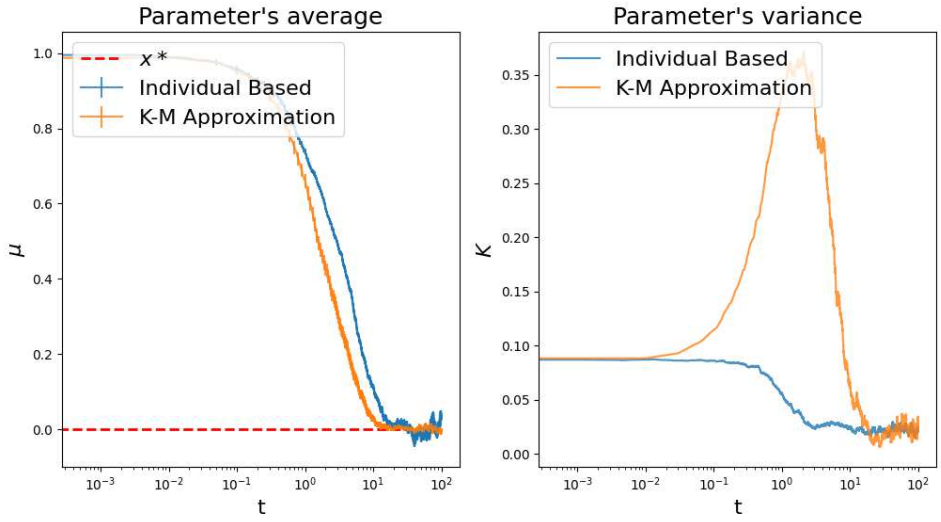

Figure 4.7: Comparison of the parameter's average μ (left panel) and variance K (right panel) between the individual based model (blue lines) and the simulated Langevin dynamics using the coefficients obtained from the Kramers-Moyal expansion of the master equation 4.17 (orange lines). These results are representative of a system composed by $M = 1000$ competitive individuals ($\nu = 0$) simulated for a period of time $t_f = 100$.

As we can see, the evolution of the average pretty much resemble the one we've found in the individual based model. However, the most noticeable difference between the two descriptions is in the evolution of the variance. Indeed, we can see that it present a peak, which was not the case in the individual based simulations. Nevertheless, even if different in the dynamics, the variance of the two models set to stationary value which is compatible between one and the other.

It is important to notice that the results just shown are based on the assumption that small "jumps" are favored by the dynamics. However, if studying the equation of the full transition rates (Eq.4.19) it is possible to notice that, actually, the favoured jumps are the one that bring the parameter as close as possible to the critical value, no matter how wide they are. In Appendix C we explore also this other approximation. We choose to report this other approximation only in the Appendix because, even though it is much more justified analytically, it produces slightly worse results.

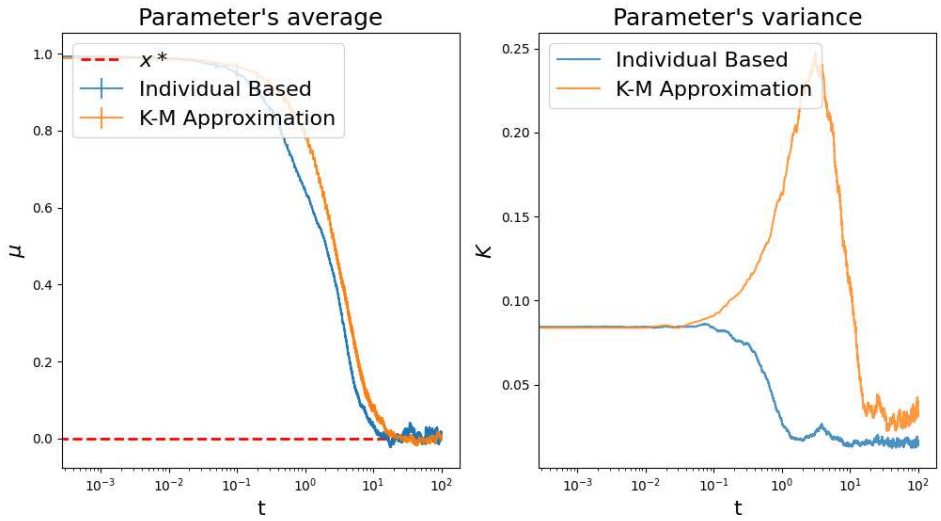

Figure 4.8: Comparison of the parameter's average μ (left panel) and variance K (right panel) between the individual based model (blue lines) and the simulated Langevin dynamics using the coefficients obtained from the Kramers-Moyal expansion of the master equation 4.17 (orange lines). These results are representative of a system composed by $M = 1000$ aggressive competitive individuals ($\nu = -1/2$) simulated for a period of time $t_f = 100$.

4.3 Strategies Dynamics and Stability

We've only considered populations in which individuals adopt all the same strategy in our analytic description until now. Like for the individual based model, we want to answer questions like: What happens if we take the optimal strategy for any specific case and introduce a small amount of individuals with different strategies? Is the previous optimal strategy still stable? In other words, the goal is obtain a set of coupled equations that describes the dynamics of both the internal parameter x and the strategy ν of an individual. In the previous *Section*, we have found an equation (Eq. 4.25) for the evolution of the internal parameter and in order to found an equation for $\dot{\nu}$ we could reference what reported in *Section* 2.2. Indeed, the transition rate

$$W(y|x) = \frac{D_{KL}^{\nu_x}(y|x)}{D_{KL}^{\nu_x}(y|x) + D_{KL}^{\nu_y}(x|y)}. \tag{4.26}$$

depends both on ν_x and ν_y and could be seen as an invasion fitness function $f(\nu_y, \nu_x)$ of an individual with strategy ν_y invading a population monomorphic for ν_x.

Therefore, adaptive dynamics of the trait ν is then given as a gradient dynamics of the invasion fitness function and described by the equation

$$\dot{\nu_x} = \frac{1}{a^2x^2}\left[ax - 2\coth(ax)\log(\cosh(ax))\right] \cdot \\ \cdot \left[a\nu_x x - (2\nu_x - 1)\coth(ax)\log(\cosh(ax))\right] \tag{4.27}$$

where the term on the right is the gradient of the invasion fitness function of a rare mutant evaluated as if it was already at criticality in the parameter internal parameter.
The latter equation together with Eq. 4.25 constitute the set of coupled equations we were looking for that completely describes our system. Furthermore, having found an equation for $\dot{\nu}$ allow us to analyze the stability of the strategies and determine their nature. First we need to check the presence of stationary strategy, i.e. strategies ν^* for which the invasion fitness function vanishes

$$\left.\frac{\partial f(\nu_y, \nu^*)}{\partial \nu_y}\right|_{\nu_y=\nu^*} = 0 \tag{4.28}$$

Without loss of generality, we could evaluate our invasion fitness function at criticality for the parameter x, i.e. at $x^* = 0$ and find which for which values of ν it vanishes. Doing so we find that the only stationary value is for $\nu = 0$. Recalling the boundary condition on ν, which are $\nu \in [-1/2, 1/2]$, we could also consider the boundaries as "stationary" point and analyze their stability too.
Following the rules explained in *Section* 2.2, we study both convergence stability and resistance to invasion of the stationary strategies. The results of this analysis are reported in Tab. 4.1.

Strategies	Stability
Neutral $\nu = 1/2$	Repelling Point
Competitive $\nu = 0$	Neutrally Stable
Aggressive $\nu = -1/2$	Resistant to Invasion

Table 4.1: Evolutionary stability analysis at the stationary points of the strategy dynamics studied at criticality in the internal parameter x.

Interestingly enough, we've found that competition, i.e. $\nu = 0$, is a neutrally stable strategy. This is due to the fact that it is resistant to invasions only from the right, which means that only individuals which adopt a strategy $\nu' < 0$ can invade a population monomophic for $\nu = 0$

since they have a higher growth rate, and it is dynamically neutral, i.e. if all individual in the systems adopt a competitive strategy and there's no perturbation of any kind the systems will stay in that configuration, however it will not converge to it spontaneously.
Regarding the boundary points, it is not possible to obtain useful information from the condition of convergence stability, since they are not stationary points in the proper sense (the first derivative does not vanishes in these points). Still, we can check if they are maxima or minima of the invasion fitness function in its domain, hence determine if they are or not resistant to invasion. Indeed, as we would have expected aggressive strategy ($\nu = -1/2$) results to be the only one which satisfies the condition of resistance to invasion, whereas neutralism ($\nu = 1/2$) happens to be a repelling point of the strategy dynamics.

5 Conclusion

With this work, we first presented some of the most recent developments in the study of critical phenomena in biology; we then identified the main characteristics of different living systems in the criticality regime and determined for which regimes these systems exhibit qualitatively different behaviour. In particular, it was observed that long-range correlations and high susceptibility to external perturbations often unite these systems. Operating in this regime could in fact bring several advantages, such as being more responsive to external stimuli and speeding up defence mechanisms against possible predators.

Faced with the fact that the literature often only shows the critical state of living systems, but without constructing a framework that formally explains how the tendency towards criticality occurs, we proposed a theoretical framework based on information theory and game theory to study these systems. Following the study of Hidalgo et al. [13], we then developed an evolutionary model in which a network of individuals interacting with each other and with the environment evolves dynamically by modifying the parameters that control each individual's representation of the external world close to a critical point.

We then have generalized the model by raising some important questions of game theory, analysing in particular what role different strategies play in the achievement of criticality by the community of individuals previously modelled. We then represented competition and aggressiveness as the tendency of an individual to exclusively maximise his own fitness while ignoring that of the group, and neutralism as the tendency of an individual to weigh equally his own fitness with respect to the one of the others.

At last, we've also proposed an analytical description based on the Langevin dynamics which have allowed us to even better characterize the tendency towards criticality that it is shown to happen in living system and study the evolutionary stability of the strategies. The result have shown that while competition and aggressiveness both pulls the population quickly to a critical point, neutralism pulls it back, however, generating much more more variability in population parameters. Still aggressive strategies in which one individual seeks to prevail over others result to be the most suitable ones and favourable.

This approach also paves the way for several future developments. For example, one possible route could be to one customarily introduce a specific trade-off between the internal parameter and the strategy in the form of a function $\nu = h(x)$ which reflects the biological fact that improvement in one "strategy" comes at the price of a loss of efficiency in the other, so that both metabolic strategies cannot be changed in an independent way. It would be interesting to investigate the evolutionary dynamics of the population constrained by a trade-off and if the system either does not diversify or diversifies into a number of coexisting species characterized by different strategies. There have already been studies ([40]-[41]-[42]) that explore a geometrical method where the evolutionary outcomes of the evolution of a monomorphic population in a 2-D phenotypic space can be characterized without specifying a particular trade-off beforehand. Referring this studies we would expect to obtain, from a study of this kind, that there exists, for some particular types of trade-offs, strategies which are branching points, i.e. strategies which are the starting point of an evolutionary diversification and speciation.

References

[1] I. E. Ohiorhenuan, F. Mechler, K. P. Purpura, A. M. Schmid, Q. Hu, and J. D. Victor, "Sparse coding and high-order correlations in fine-scale cortical networks," *Nature*, vol. 466, no. 7306, pp. 617–621, July 2010. [Online]. Available: https://ideas.repec.org/a/nat/nature/v466y2010i7306d10.1038_nature09178.html

[2] A. Cavagna, A. Cimarelli, I. Giardina, G. Parisi, R. Santagati, F. Stefanini, and M. Viale, "Scale-free correlations in starling flocks," *Proceedings of the National Academy of Sciences*, vol. 107, no. 26, pp. 11 865–11 870, 2010. [Online]. Available: https://www.pnas.org/doi/abs/10.1073/pnas.1005766107

[3] H. Chaté and M. Muñoz, "Insect swarms go critical," *Physics*, vol. 7, 11 2014.

[4] T. Mora and W. Bialek, "Are biological systems poised at criticality?" *Journal of Statistical Physics*, vol. 144, pp. 268–302, 07 2011. [Online]. Available: https://doi.org/10.1007/s10955-011-0229-4

[5] J. M. Beggs and D. Plenz, "Neuronal avalanches in neocortical circuits," *Journal of Neuroscience*, vol. 23, no. 35, pp. 11 167–11 177, 2003. [Online]. Available: https://www.jneurosci.org/content/23/35/11167

[6] M. Nykter, N. D. Price, M. Aldana, S. A. Ramsey, S. A. Kauffman, L. E. Hood, O. Yli-Harja, and I. Shmulevich, "Gene expression dynamics in the macrophage exhibit criticality," *Proceedings of the National Academy of Sciences*, vol. 105, no. 6, pp. 1897–1900, 2008. [Online]. Available: https://www.pnas.org/doi/abs/10.1073/pnas.0711525105

[7] C. Furusawa and K. Kaneko, "Adaptation to optimal cell growth through self-organized criticality," *Phys. Rev. Lett.*, vol. 108, p. 208103, May 2012. [Online]. Available: https://link.aps.org/doi/10.1103/PhysRevLett.108.208103

[8] D. Krotov, J. O. Dubuis, T. Gregor, and W. Bialek, "Morphogenesis at criticality," *Proceedings of the National Academy of Sciences*, vol. 111, no. 10, pp. 3683–3688, 2014. [Online]. Available: https://www.pnas.org/doi/abs/10.1073/pnas.1324186111

[9] X. Chen, X. Dong, A. Be'er, H. L. Swinney, and H. P. Zhang, "Scale-invariant correlations in dynamic bacterial clusters," *Phys. Rev. Lett.*, vol. 108, p. 148101, Apr 2012. [Online]. Available: https://link.aps.org/doi/10.1103/PhysRevLett.108.148101

[10] W. Bialek, A. Cavagna, I. Giardina, T. Mora, E. Silvestri, M. Viale, and A. M. Walczak, "Statistical mechanics for natural flocks of birds," *Proceedings of the National Academy of Sciences*, vol. 109, no. 13, pp. 4786–4791, 2012. [Online]. Available: https://www.pnas.org/doi/abs/10.1073/pnas.1118633109

[11] O. G. Mouritsen, "Introduction to phase transitions and critical phenomena. by h. eugene stanley, oxford university press, oxford, 1987," *International Journal of Quantum Chemistry*, vol. 35, no. 4, pp. 583–584, 1989. [Online]. Available: https://onlinelibrary.wiley.com/doi/abs/10.1002/qua.560350412

[12] J. Binney, N. Dowrick, A. Fisher, and M. Newman, *The Theory of Critical Phenomena: An Introduction to the Renormalization Group*, ser. Oxford Science Publ. Clarendon Press, 1992. [Online]. Available: https://books.google.it/books?id=lvZcGJI3X9cC

[13] J. Hidalgo, J. Grilli, S. Suweis, M. A. Muñoz, J. R. Banavar, and A. Maritan, "Information-based fitness and the emergence of criticality in living systems," *Proceedings of the National Academy of Sciences*, vol. 111, no. 28, pp. 10095–10100, 2014. [Online]. Available: https://www.pnas.org/doi/abs/10.1073/pnas.1319166111

[14] J. Hidalgo, J. Grilli, S. Suweis, A. Maritan, and M. A. Muñoz, "Cooperation, competition and the emergence of criticality in communities of adaptive systems," *Journal of Statistical Mechanics: Theory and Experiment*, vol. 2016, no. 3, p. 033203, mar 2016. [Online]. Available: https://dx.doi.org/10.1088/1742-5468/2016/03/033203

[15] E. Schrödinger, *What is Life?* Cambridge University Press, 1967.

[16] R. Livi and P. Politi, *Nonequilibrium Statistical Physics: A Modern Perspective*. Cambridge University Press, 2017.

[17] P. Bak, C. Tang, and K. Wiesenfeld, "Self-organized criticality: An explanation of the 1/f noise," *Phys. Rev. Lett.*, vol. 59, pp. 381–384, Jul 1987. [Online]. Available: https://link.aps.org/doi/10.1103/PhysRevLett.59.381

[18] P. Bak and C. Tang, "Earthquakes as a self-organized critical phenomenon," *Journal of Geophysical Research: Solid Earth*, vol. 94, no. B11, pp. 15 635–15 637, 1989. [Online]. Available: https://agupubs.onlinelibrary.wiley.com/doi/abs/10.1029/JB094iB11p15635

[19] P. Bak, K. Chen, and C. Tang, "A forest-fire model and some thoughts on turbulence," *Physics Letters A*, vol. 147, no. 5, pp. 297–300, 1990. [Online]. Available: https://www.sciencedirect.com/science/article/pii/037596019090451S

[20] M. A. Muñoz, "Colloquium: Criticality and dynamical scaling in living systems," *Rev. Mod. Phys.*, vol. 90, p. 031001, Jul 2018. [Online]. Available: https://link.aps.org/doi/10.1103/RevModPhys.90.031001

[21] E. Tagliazucchi, P. Balenzuela, D. Fraiman, and D. Chialvo, "Criticality in large-scale brain fmri dynamics unveiled by a novel point process analysis," *Frontiers in Physiology*, vol. 3, 2012. [Online]. Available: https://www.frontiersin.org/articles/10.3389/fphys.2012.00015

[22] G. De Palo, D. Yi, and R. G. Endres, "A critical-like collective state leads to long-range cell communication in dictyostelium discoideum aggregation," *PLOS Biology*, vol. 15, no. 4, pp. 1–25, 04 2017. [Online]. Available: https://doi.org/10.1371/journal.pbio.1002602

[23] G. Deco and V. K. Jirsa, "Ongoing cortical activity at rest: Criticality, multistability, and ghost attractors," *Journal of Neuroscience*, vol. 32, no. 10, pp. 3366–3375, 2012. [Online]. Available: https://www.jneurosci.org/content/32/10/3366

[24] J. A. Edlund, N. Chaumont, A. Hintze, C. Koch, G. Tononi, and C. Adami, "Integrated information increases with fitness in the evolution of animats," *PLOS Computational Biology*, vol. 7, no. 10, pp. 1–13, 10 2011. [Online]. Available: https://doi.org/10.1371/journal.pcbi.1002236

[25] A. Haimovici, E. Tagliazucchi, P. Balenzuela, and D. R. Chialvo, "Brain organization into resting state networks emerges at criticality on a model of the human connectome,"

Phys. Rev. Lett., vol. 110, p. 178101, Apr 2013. [Online]. Available: https://link.aps.org/doi/10.1103/PhysRevLett.110.178101

[26] D. R. Chialvo, "Emergent complex neural dynamics," *Nature Physics*, vol. 6, pp. 744–750, 2010. [Online]. Available: https://doi.org/10.1038/nphys1803

[27] A. M. Turing, "I.—Computing machinery and intelligence," *Mind*, vol. LIX, no. 236, pp. 433–460, 10 1950. [Online]. Available: https://doi.org/10.1093/mind/LIX.236.433

[28] W. Ashby, *Design for a Brain. The origin of adaptive behaviour citation*. Wiley, New York, 1960.

[29] R. V. Solé and O. Miramontes, "Information at the edge of chaos in fluid neural networks," *Physica D: Nonlinear Phenomena*, vol. 80, no. 1, pp. 171–180, 1995. [Online]. Available: https://www.sciencedirect.com/science/article/pii/0167278995900756

[30] J. T. Lizier, M. Prokopenko, and A. Y. Zomaya, "Local information transfer as a spatiotemporal filter for complex systems," *Phys. Rev. E*, vol. 77, p. 026110, Feb 2008. [Online]. Available: https://link.aps.org/doi/10.1103/PhysRevE.77.026110

[31] X. R. Wang, J. T. Lizier, and M. Prokopenko, "Fisher Information at the Edge of Chaos in Random Boolean Networks," *Artificial Life*, vol. 17, no. 4, pp. 315–329, 10 2011. [Online]. Available: https://doi.org/10.1162/artl_a_00041

[32] P. Krawitz and I. Shmulevich, "Basin entropy in boolean network ensembles," *Phys. Rev. Lett.*, vol. 98, p. 158701, Apr 2007. [Online]. Available: https://link.aps.org/doi/10.1103/PhysRevLett.98.158701

[33] T. M. Cover, J. A. Thomas, and J. Wiley, *Elements of Information Theory*. John Wiley & Sons, Ltd, 1991.

[34] J. M. Smith and G. Price, "The logic of animal conflict," *Nature*, vol. 246, pp. 15–18, nov 1973. [Online]. Available: https://doi.org/10.1038/246015a0

[35] B. J. McGill and J. S. Brown, "Evolutionary game theory and adaptive dynamics of continuous traits," *Annual Review of Ecology, Evolution, and Systematics*, vol. 38, pp. 403–435, 2007. [Online]. Available: http://www.jstor.org/stable/30033866

[36] M. Doebeli and I. Ispolatov, "Continuously stable strategies as evolutionary branching points," *Journal of Theoretical Biology*, vol. 266, no. 4, pp. 529–535, oct 2010. [Online]. Available: https://doi.org/10.1016%2Fj.jtbi.2010.06.036

[37] D. Dean, "Langevin equation for the density of a system of interacting langevin processes," *Journal of Physics A: Mathematical and General*, vol. 29, no. 24, p. L613, dec 1996. [Online]. Available: https://dx.doi.org/10.1088/0305-4470/29/24/001

[38] H. Kramers, "Brownian motion in a field of force and the diffusion model of chemical reactions," *Physica*, vol. 7, no. 4, pp. 284–304, 1940. [Online]. Available: https://www.sciencedirect.com/science/article/pii/S0031891440900982

[39] J. Moyal, "Stochastic processes and statistical physics," *Journal of the Royal Statistical Society. Series B (Methodological)*, vol. 11, no. 2, pp. 150–210, 1949. [Online]. Available: http://www.jstor.org/stable/2984076

[40] C. de Mazancourt and U. Dieckmann, "Trade-off geometries and frequency-dependent selection," *American Naturalist - AMER NATURALIST*, vol. 164, pp. 765–778, 12 2004.

[41] C. Rueffler, T. J. M. Van Dooren, and J. A. J. Metz, "Adaptive walks on changing landscapes: Levins' approach extended." *Theoretical population biology*, vol. 65, pp. 165–78, Mar 2004.

[42] R. Bowers, A. Hoyle, A. White, and M. Boots, "The geometric theory of adaptive evolution: trade-off and invasion plots." *Journal of theoretical biology*, vol. 233, pp. 363–77, 2005.

Acknowledgments

I am grateful to prof. Maritan and prof. Suweis for helpful discussions and constant support. I would also like to thank F. Menegazzo for the valuable suggestions and help during the realization of this project.

A

Non-stable Solution

Consider two individual agents i and j — the source for i is j and vice versa — each of them with its own probabilistic gene network. The relative fitnesses of i and j are determined by how well the set of cues (described by the probability distribution $P(\boldsymbol{s}|\boldsymbol{x})$) of one organism is captured by the other with minimum information loss, and vice versa (for simplicity, we could assume that the distributions associated with i and j correspond to equilibrium distributions of an Ising model at similar inverse temperatures x_i and x_j). If $x_i = x_j$, the two distributions would be identical and the KL divergence would vanish. However, this is not a stable solution. Indeed, if the two parameters are not identical but close, the difference between their respective KL divergences from each to the other is

$$D_{KL}(x+\delta x|x) - D_{KL}(x|x+\delta x) \simeq \frac{1}{6}\nabla\chi(x)\delta x^3 \tag{A.1}$$

To prove this let us start by writing explicitly the KL divergences using the definition:

$$D_{KL}(x+\delta x|x) = \sum_s P(s|x+\delta x)\log\left(\frac{P(s|x+\delta x)}{P(s|x)}\right) \tag{A.2}$$

$$D_{KL}(x|x+\delta x) = -\sum_s P(s|x)\log\left(\frac{P(s|x+\delta x)}{P(s|x)}\right) \tag{A.3}$$

Since δx is small, we can expand $P(s|x+\delta x)$ around x, namely

$$P(s|x+\delta x) = P(s|x) + \delta x \partial_x P(s|x) + \frac{1}{2}\delta x \partial_x^2 P(s|x) + \frac{1}{6}\delta x^3 \partial_x^3 P(s|x) \tag{A.4}$$

$$= P(s|x)\left[1 + \Delta\phi\delta x + \frac{\delta x^2}{2}\left(\Delta\phi^2 - \chi(x)\right) + \frac{\delta x^3}{6}\left(\Delta\phi^3 - 3\Delta\phi\chi(x) - \nabla\chi(x)\right)\right] \tag{A.5}$$

where $\Delta\phi = \langle\phi\rangle_x - \phi$ and $\chi(x) = \langle\phi^2\rangle - \langle\phi\rangle^2$. Inserting this expansion in the definition given above we arrive at

$$D_{KL}(x+\delta x|x) = \sum_s P(s|x)[1+\dots]\log[1+\dots] \tag{A.6}$$

$$D_{KL}(x|x+\delta x) = -\sum_s P(s|x)\log[1+\dots] \tag{A.7}$$

where the term under parenthesis $[1+\dots]$ is the one of Eq. A.5. Proceeding furthermore with the expansion of the logarithm

$$\log\left[1 + \Delta\phi\delta x + \frac{\delta x^2}{2}\left(\Delta\phi^2 - \chi(x)\right) + \frac{\delta x^3}{6}\left(\Delta\phi^3 - 3\Delta\phi\chi(x) - \nabla\chi(x)\right)\right] \simeq \tag{A.8}$$

$$\simeq \Delta\phi\delta x - \frac{1}{2}\chi(x)\delta x^2 - \frac{1}{6}\nabla\chi(x)\delta x^3 \tag{A.9}$$

and exploiting everything up to 3^{rd} order in δx in Eq. A.2 and Eq. A.3, we arrive at

$$D_{KL}(x+\delta x|x) \simeq \frac{\delta x^2}{2}\chi(x) + \frac{\delta x^3}{3}\nabla\chi(x) \tag{A.10}$$

$$D_{KL}(x|x+\delta x) \simeq \frac{\delta x^2}{2}\chi(x) + \frac{\delta x^3}{6}\nabla\chi(x) \tag{A.11}$$

By subtracting them we obtain the initial statement

$$D_{KL}(x+\delta x|x) - D_{KL}(x|x+\delta x) \simeq \frac{1}{6}\nabla\chi(x)\delta x^3, \tag{A.12}$$

therefore proving it.

B

Derivation of the equation for the evolution of the density using Dean's method

In this appendix we briefly review the calculation done by Dean [37] to obtain a dynamical equation for the density of a system of interacting "particles" each one obeying a Langevin dynamics.
Any function of the form $f(\boldsymbol{x}^i)$ can be written as

$$f(\boldsymbol{x}^i) = \int \mathrm{d}\boldsymbol{x}\, \rho^i(\boldsymbol{x}, t) f(\boldsymbol{x}) \tag{B.1}$$

where $\rho^i(\boldsymbol{x}, t) = \delta(\boldsymbol{x} - \boldsymbol{x}^i(t))$ is the contribution of each individual i to the global distribution of parameters, and its time derivative is

$$\frac{\mathrm{d}f(\boldsymbol{x}^i)}{\mathrm{d}t} = \int \mathrm{d}\boldsymbol{x}\, \frac{\partial \rho^i(\boldsymbol{x}, t)}{\partial t} f(\boldsymbol{x}) \tag{B.2}$$

However, we can find another expression for the time derivative of $f(\boldsymbol{x}^i)$ using the Ito's calculus.
Consider the Ito process

$$\mathrm{d}X_t = a(X_t, t)\, \mathrm{d}t + b(X_t, t)\, \mathrm{d}W_t \tag{B.3}$$

and a continuos differentianble (at least twice) function $f(X_t)$, then the Ito's Lemma states

$$\mathrm{d}f = \frac{\partial f}{\partial X_t}\,\mathrm{d}X_t + \frac{1}{2}\frac{\partial^2 f}{\partial X_t^2}\,(\mathrm{d}X_t)^2 \tag{B.4}$$

Inserting eq. (B.3) in the latter one

$$\begin{aligned} df &= \frac{\partial f}{\partial X_t}\,\mathrm{d}X_t + \frac{1}{2}\frac{\partial^2 f}{\partial X_t^2}\,(\mathrm{d}X_t)^2 \\ &= \frac{\partial f}{\partial X_t}\,(a_t\,\mathrm{d}t + b_t\,\mathrm{d}W_t) + \frac{1}{2}\frac{\partial^2 f}{\partial X_t^2}\,(a_t\,\mathrm{d}t + b_t\,\mathrm{d}W_t)^2 \\ &= \left(\frac{\partial f}{\partial X_t}a_t + \frac{1}{2}\frac{\partial^2 f}{\partial X_t^2}b_t^2\right)\mathrm{d}t + \frac{\partial f}{\partial X_t}b_t\,\mathrm{d}W_t \end{aligned} \tag{B.5}$$

In the case under study $a_t = -\frac{1}{N}\sum_{j=1}^{N}\nabla_x V(D(\boldsymbol{x}^j(t),\boldsymbol{x}))$, $b_t = \sqrt{2T}$ and $\mathrm{d}W_t = \boldsymbol{\eta}^i(t)\,\mathrm{d}t$. Hence, we arrive at a new expression for the time derivative of $f(\boldsymbol{x}^i)$, namely

$$\frac{\mathrm{d}f(\boldsymbol{x}^i)}{\mathrm{d}t} = \int \mathrm{d}\boldsymbol{x}\,\rho^i(\boldsymbol{x},t)\left(\nabla_{\boldsymbol{x}} f(\boldsymbol{x})\cdot\left(\sqrt{2T}\boldsymbol{\eta}^i(t) - \frac{1}{N}\sum_{j=1}^{N}\nabla_{\boldsymbol{x}} V(D(\boldsymbol{x}^j(t),\boldsymbol{x}))\right) + T\nabla_{\boldsymbol{x}}^2 f(\boldsymbol{x})\right) \tag{B.6}$$

Integrating by part and comparing with eq. (B.2), we arrive at

$$\begin{aligned} \frac{\partial\rho^i(\boldsymbol{x},t)}{\partial t} = -\sqrt{2T}\nabla_{\boldsymbol{x}}\cdot\left(\rho^i(\boldsymbol{x},t)\boldsymbol{\eta}^i(t)\right) + \nabla_{\boldsymbol{x}}\cdot\left(\rho^i(\boldsymbol{x},t)\left(\frac{1}{N}\sum_{j=1}^{N}\nabla_{\boldsymbol{x}} V(D(\boldsymbol{x}^j(t),\boldsymbol{x}))\right)\right) + \\ + T\nabla_{\boldsymbol{x}}^2\rho^i(\boldsymbol{x},t) \end{aligned} \tag{B.7}$$

This equation is almost a closed equation for ρ, the problem is that the noise term appears to contain too much information about the individual ρ^i and hence, in the current form, is not a Markovian equation for the evolution of the global density.
We can define a new delta-correlated Gaussian noise as

$$\boldsymbol{\eta}'(\boldsymbol{x},t) = N^{-1/2}\nabla_{\boldsymbol{x}}\cdot(\boldsymbol{\xi}(\boldsymbol{x},t)\rho^{1/2}(\boldsymbol{x},t)) \tag{B.8}$$

where $\boldsymbol{\xi}(\boldsymbol{x},t)$ is a global uncorrelated white noise field such that $\langle\xi^\mu(\boldsymbol{x},t)\xi^\nu(\boldsymbol{y},t'\rangle = \delta_{\mu\nu}\delta(\boldsymbol{x}-\boldsymbol{y})\delta(t-t')$. This new noise has the same correlation function as the previous one, hence we can replace the term $-1/N\sum_{i=1}^{N}\nabla_{\boldsymbol{x}}\cdot(\rho^i(\boldsymbol{x},t)\boldsymbol{\eta}^i(t))$ with it and averaging over individuals

we obtain

$$\frac{\partial \rho(\boldsymbol{x},t)}{\partial t} = \sqrt{\frac{2T}{N}} \nabla_{\boldsymbol{x}} \cdot \left(\sqrt{\rho(\boldsymbol{x},t)} \boldsymbol{\xi}(\boldsymbol{x},t) \right) + T \nabla^2_{\boldsymbol{x}} \rho(\boldsymbol{x},t) + \\ + \nabla_{\boldsymbol{x}} \cdot \left(\rho(\boldsymbol{x},t) \left(\frac{1}{N} \sum_{j=1}^{N} \nabla_{\boldsymbol{x}} V(D(\boldsymbol{x}^j(t), \boldsymbol{x})) \right) \right) \tag{B.9}$$

Employing what found, it is possible derive a set of deterministic equations for the evolution of its moments for $N \to \infty$. The mean $\mu(t) = \int \mathrm{d}\boldsymbol{x}\, \rho(\boldsymbol{x},t)\, \boldsymbol{x}$ can be obtained multiplying by $\boldsymbol{x}$ and integrating by parts

$$\begin{aligned} \dot{\mu}_\alpha(t) &= \int \mathrm{d}\boldsymbol{x}\, \partial_t \rho(\boldsymbol{x},t)\, x_\alpha \\ &= -\int \mathrm{d}\boldsymbol{x}\, \nabla_{\boldsymbol{x}} \cdot \left(\rho(\boldsymbol{x},t) \int \mathrm{d}\boldsymbol{y}\, \rho(\boldsymbol{y},t) \boldsymbol{F}(\boldsymbol{y},\boldsymbol{x}) \right) x_\alpha + T \int \mathrm{d}\boldsymbol{x}\, \nabla^2_{\boldsymbol{x}} \rho(\boldsymbol{x},t)\, x_\alpha \\ &= \int \mathrm{d}\boldsymbol{x}\, \rho(\boldsymbol{x},t) \int \mathrm{d}\boldsymbol{y}\, \rho(\boldsymbol{y},t) F_\alpha(\boldsymbol{y},\boldsymbol{x}) - \underbrace{T \int \mathrm{d}\boldsymbol{x}\, \nabla_{\boldsymbol{x}} \rho(\boldsymbol{x},t)}_{\to 0} \\ &= \int \mathrm{d}\boldsymbol{x}\, \rho(\boldsymbol{x},t) \int \mathrm{d}\boldsymbol{y}\, \rho(\boldsymbol{y},t) F_\alpha(\boldsymbol{y},\boldsymbol{x}) \end{aligned} \tag{B.10}$$

Similarly, for the covariance matrix $K_{\alpha\beta} = \int \mathrm{d}\boldsymbol{x}\, \rho(\boldsymbol{x},t)(x_\alpha - \mu_\alpha(t))(x_\beta - \mu_\beta(t))$

$$\begin{aligned} \dot{K}_{\alpha\beta} &= \int \mathrm{d}\boldsymbol{x}\, \partial_t \rho(\boldsymbol{x},t)(x_\alpha - \mu_\alpha(t))(x_\beta - \mu_\beta(t)) \\ &= -\int \mathrm{d}\boldsymbol{x}\, \nabla_{\boldsymbol{x}} \cdot \left(\rho(\boldsymbol{x},t) \int \mathrm{d}\boldsymbol{y}\, \rho(\boldsymbol{y},t) \boldsymbol{F}(\boldsymbol{y},\boldsymbol{x}) \right) (x_\alpha - \mu_\alpha)(x_\beta - \mu_\beta) \\ &\quad + T \int \mathrm{d}\boldsymbol{x}\, \nabla^2_{\boldsymbol{x}} \rho(\boldsymbol{x},t)(x_\alpha - \mu_\alpha)(x_\beta - \mu_\beta) \\ &= 2T \int \mathrm{d}\boldsymbol{x}\, \rho(\boldsymbol{x},t) \delta_{\alpha\beta} + \left[\int \mathrm{d}\boldsymbol{x} \left(\int \mathrm{d}\boldsymbol{y}\, \rho(\boldsymbol{y},t) F_\beta(\boldsymbol{y},\boldsymbol{x}) \right) (x_\alpha - \mu_\alpha) \right. \\ &\qquad \left. + \int \mathrm{d}\boldsymbol{x} \left(\int \mathrm{d}\boldsymbol{y}\, \rho(\boldsymbol{y},t) F_\alpha(\boldsymbol{y},\boldsymbol{x}) \right) (x_\beta - \mu_\beta) \right] \\ &= 2T\delta_{\alpha\beta} + \sum_{\gamma,\varepsilon=1}^{d} (\delta_{\alpha\gamma}\delta_{\beta\varepsilon} + \delta_{\alpha\varepsilon}\delta_{\beta\gamma}) \int \mathrm{d}\boldsymbol{x}\, \rho(\boldsymbol{x},t)(x_\gamma - \mu_\gamma) \int \mathrm{d}\boldsymbol{y}\, \rho(\boldsymbol{y},t) F_\varepsilon(\boldsymbol{y},\boldsymbol{x}) \end{aligned} \tag{B.11}$$

C

Gaussian Approximation of the Fitness

We observe in Fig. C.1 that the transition rates $W(y|x)$ as a function of y have Gaussian-like shapes. Moreover, we notice that the maximum, even though it slightly depends on the value of x, stays in the vicinity of the critical value $y = 0$, meaning that changes in the internal parameter are much more likely to happen towards the critical value than towards the value of other individuals' parameter. Hence, we can expand $\log[W(y|x)]$ around $y = 0$ finding, therefore, a quadratic form for the transition rates, namely

$$W(y|x) \simeq W(0|x) \exp\{-\alpha_2 y^2 + \alpha_1 y\} \tag{C.1}$$

where the coefficients α_1 and α_2, actually, depend on x and ν.
For completeness, we report the expressions and of the coefficients obtained through the expansion

$$W(0|x) = \frac{\nu - (2\nu - 1)\coth(ax)\log(\cosh(ax))}{ax} \tag{C.2}$$

$$\alpha_1 = -\frac{(2\nu - 1)\coth(ax)\left(-a^2x^2 + \log(\cosh(ax)) + ax\coth(ax)\log(\cosh(ax))\right)}{x(a\nu x - (2\nu - 1)\coth(ax)\log(\cosh(ax)))} \tag{C.3}$$

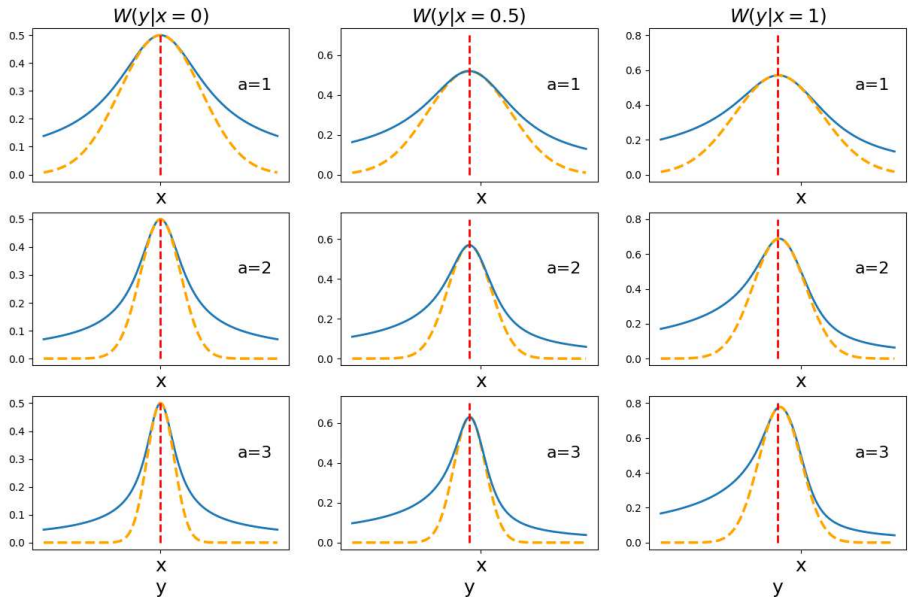

Figure C.1: Plots of the transition rates (for $\nu = 0$) $W(y|x)$ (solid blue lines) and their approximation as quadratic form in $y = 0$ (scattered orange lines) for different values of x (columns) and different values of the sharpening parameter a (rows). The vertical scattered red lines represent $y = 0$.

$$\begin{aligned}\alpha_2 \;=\; \coth(ax)\Bigg(&\frac{-2a^3\nu(2\nu-1)x^3\coth^2(ax)\log(\cosh(ax))}{2x^2(a\nu x-(2\nu-1)\coth(ax)\log(\cosh(ax)))^2}+\\&+\frac{a(2\nu-1)\nu x\left(a^2x^2-2\log(\cosh(ax))\right)}{2x^2(a\nu x-(2\nu-1)\coth(ax)\log(\cosh(ax)))^2}\\&+\frac{a^2(1-2\nu)^2x^2\coth^3(ax)\log^2(\cosh(ax))}{2x^2(a\nu x-(2\nu-1)\coth(ax)\log(\cosh(ax)))^2}\\&+\frac{(2\nu-1)\coth(ax)\left(a^4x^4-a^2x^2\log(\cosh(ax))\right)}{2x^2(a\nu x-(2\nu-1)\coth(ax)\log(\cosh(ax)))^2}\\&+\frac{(2\nu-1)\log^2(\cosh(ax))}{2x^2(a\nu x-(2\nu-1)\coth(ax)\log(\cosh(ax)))^2}\Bigg)\end{aligned}\tag{C.4}$$

Since the the expression of the transition rate and, conversely, the expression of its quadratic form diverge for values of x in the vicinity of $x^* = 0$, it is worth pointing out the quadratic form in the limit $x \to 0$, which is finite and have the following expression

$$\log W(y|0) \simeq -\log 2 + \frac{1}{6}a^2(2\nu-1)y^2. \tag{C.5}$$

With this approximation we can perform the integral in Eq. 4.21 exactly since it reduces to a Gaussian integral, hence we obtain that the drift coefficient expression become

$$\begin{aligned} A_1(x) &= \int \mathrm{d}y\,(y-x)W(0|x)e^{-\alpha_2 y^2+\alpha_1 y} \\ &= W(0|x)\sqrt{\frac{\pi}{\alpha_2}}e^{\frac{\alpha_1^2}{4\alpha_2}}\left[\frac{\alpha_1}{2\alpha_2}-x\right] \end{aligned} \tag{C.6}$$

and the one for the diffusion coefficient become

$$\begin{aligned} A_2(x) &= \int \mathrm{d}y\,(y-x)^2W(0|x)e^{-\alpha_2 y^2+\alpha_1 y} \\ &= W(0|x)\sqrt{\frac{\pi}{\alpha_2}}e^{\frac{\alpha_1^2}{4\alpha_2}}\left[\frac{1}{2\alpha_2}+\left(\frac{\alpha_1}{2\alpha_2}-x\right)^2\right] \end{aligned} \tag{C.7}$$

Having an expression for the drift coefficient, $A_1(x)$, and for the diffusion coefficient, $A_2(x)$, let us now write the Langevin equation associated to the Fokker-Plank equation 4.20, which reads

$$\mathrm{d}x\,(t) = A_1(x)\,\mathrm{d}t + \sqrt{A_2(x)}\,\mathrm{d}\eta\,(t) \tag{C.8}$$

where $\eta(t)$ is the stochastic variable characterised by $\langle\eta(t)\rangle = 0$ and $\langle\eta(t)\eta(t')\rangle = \delta(t-t')$.

Figure C.2 and C.3 show the results obtained with the latter Langevin equation. The Gaussian approximation actually give us pretty good results. Indeed, the form of the approximated transition rate using the Gaussian approximation is much more close to the complete one than the approximation used in the main text. However, as we can see, given the complexity of the coefficients in this expansions we run into some issue. The most noticeable are in the parameter's variance which is not compatible to what we've found in the individual based model (*Chapter* 3). Moreover, as the system reach criticality, the parameter's variance exhibits more and more spikes which are probably due to some numerical nuances, since we do not see this much variability in the dispersion of the means.
For these reasons we've decided to report this approximation only as an appendix even though the assumptions made are much more reasonable and rigorous than the assumptions made for the approximation in the main text.

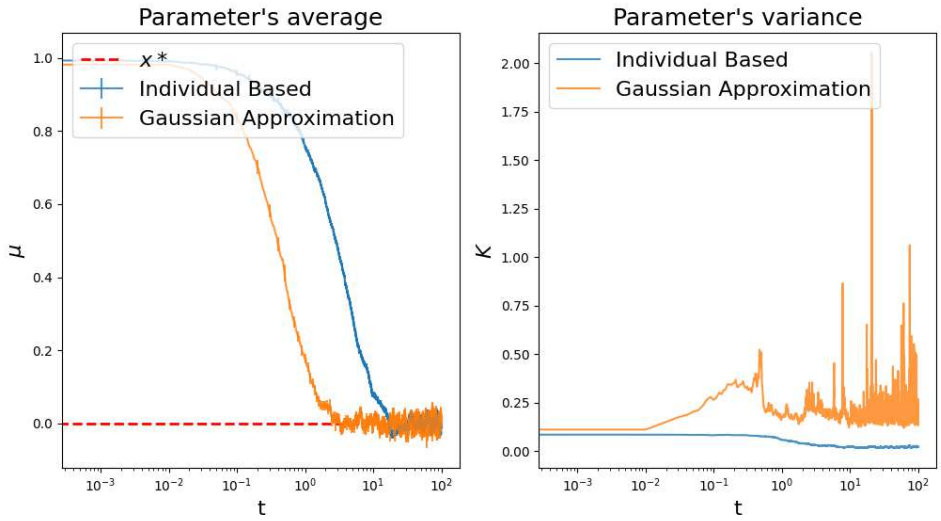

Figure C.2: Comparison of the parameter's average μ (left panel) and variance K (right panel) between the individual based model (blue lines) and the simulated Langevin dynamics using the coefficients obtained from the Kramers-Moyal expansion of the master equation 4.17 (orange lines) in the Gaussian approximation. These results are representative of a system composed by $M = 1000$ competitive individuals ($\nu = 0$) simulated for a period of time $t_f = 100$.

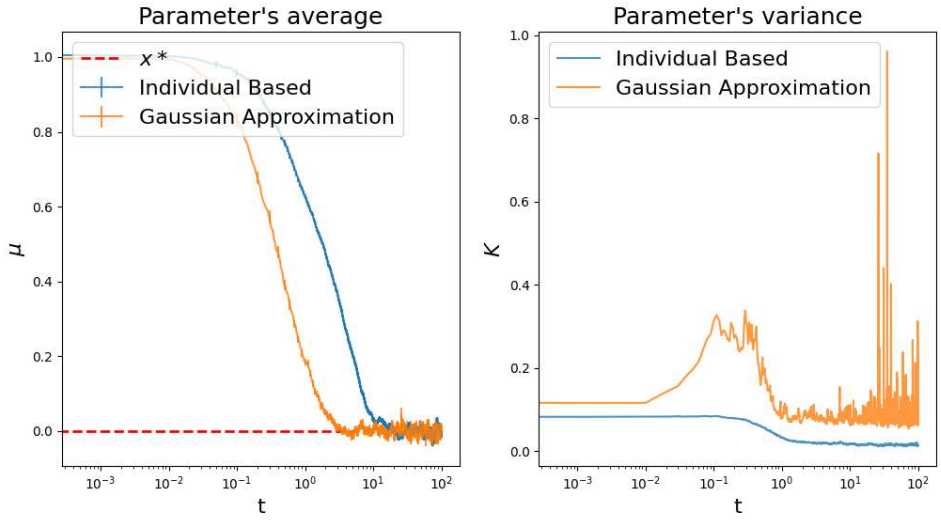

Figure C.3: Comparison of the parameter's average μ (left panel) and variance K (right panel) between the individual based model (blue lines) and the simulated Langevin dynamics using the coefficients obtained from the Kramers-Moyal expansion of the master equation 4.17 (orange lines) in the Gaussian approximation. These results are representative of a system composed by $M = 1000$ aggressive competitive individuals ($\nu = -1/2$) simulated for a period of time $t_f = 100$.